

การพัฒนาวิธีสเปกตรัมเชิงกำหนดสำหรับการแก้
สมการจลน์โบลต์มันน์ไม่เชิงเส้น

นายชัชวาลย์ วัชรารื่องวิทย์

วิทยานิพนธ์นี้เป็นส่วนหนึ่งของการศึกษาตามหลักสูตรปริญญาวิทยาศาสตรดุษฎีบัณฑิต
สาขาวิชาคณิตศาสตร์ประยุกต์
มหาวิทยาลัยเทคโนโลยีสุรนารี
ปีการศึกษา 2550

**DEVELOPMENT OF A DETERMINISTIC
SPECTRAL METHOD FOR SOLVING
THE NONLINEAR BOLTZMANN
KINETIC EQUATION**

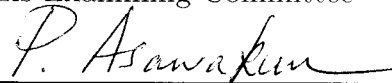
Chatchawan Watchararuangwit

**A Thesis Submitted in Partial Fulfillment of the Requirements for the
Degree of Doctor of Philosophy in Applied Mathematics
Suranaree University of Technology
Academic Year 2007**

**DEVELOPMENT OF A DETERMINISTIC SPECTRAL
METHOD FOR SOLVING THE NONLINEAR
BOLTZMANN KINETIC EQUATION**

Suranaree University of Technology has approved this thesis submitted in
partial fulfillment of the requirements for the Degree of Doctor of Philosophy.

Thesis Examining Committee



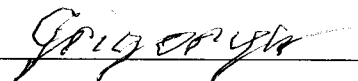
(Assoc. Prof. Dr. Prapasri Asawakun)

Chairperson



(Prof. Dr. Sergey Meleshko)

Member (Thesis Advisor)



(Prof. Dr. Yurii Grigoriev)

Member



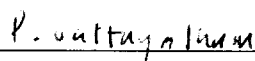
(Assoc. Prof. Dr. Nikolay Moshkin)

Member



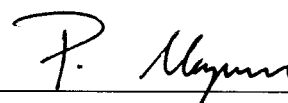
(Asst. Prof. Dr. Eckart Schulz)

Member



(Prof. Dr. Pairote Sattayatham)

Vice Rector for Academic Affairs



(Assoc. Prof. Dr. Prapan Manyum)

Dean of Institute of Science

ชัชวาลย์ วัชรารื่องวิทย์ : การพัฒนาวิธีสเปกตรัมเชิงกำหนดสำหรับการแก้สมการจลน์
โบลต์ซมันน์ไม่เชิงเส้น (DEVELOPMENT OF A DETERMINISTIC SPECTRAL
METHOD FOR SOLVING THE NONLINEAR BOLTZMANN KINETIC
EQUATION) อาจารย์ที่ปรึกษา : ศาสตราจารย์ ดร. เซอร์เก เมเลซโก, 77 หน้า.

งานวิจัยนี้ได้พัฒนาวิธีใหม่สำหรับแก้สมการจลน์ของโบลต์ซมันน์ในกรณีโมเลกุลแมกซ์-
เวลล์ ซึ่งมีสมมาตรทรงกระบอกในตัวแปรความเร็ว โดยใช้วิธีแบ่งตามกระบวนการเชิงกายภาพ
ทำให้สมการโบลต์ซมันน์ได้แยกออกเป็นสมการโบลต์ซมันน์เอกพันธ์และสมการการถ่ายเท การ
แก้สมการการถ่ายเทได้ใช้แบบแผนของแล็กซ์-เวนครอฟฟ์หรืออัปวินด์ การแปลงฟูริเยร์บนปริภูมิ
ความเร็วทำให้สมการโบลต์ซมันน์เอกพันธ์ง่ายขึ้นสำหรับแบบจำลองแมกซ์เวลล์ เนื่องจากปัญหา
มีสมมาตรทรงกระบอกจึงทำให้ การแปลงฟูริเยร์ 3 มิติสมนัยกับการแปลงฟูริเยร์ 1 มิติ และการ
แปลงแอนเคล การใช้เอกซ์โปเนนเชียลกริดในปริภูมิความเร็วทำให้สามารถใช้ประสิทธิภาพของ
ขั้นตอนวิธีการแปลงฟูริเยร์แบบเร็วได้ การแก้สมการโบลต์ซมันน์เอกพันธ์ในปริภูมิฟูริเยร์ได้ใช้วิธี
รุงเง-คุททา วิธีใหม่ที่พัฒนาขึ้นในงานวิจัยนี้ได้นำไปประยุกต์ในการแก้ปัญหาค่าการถ่ายเทความร้อน
และรีคอนเด้นเซชันระหว่างแผ่นขนาน

สาขาวิชาคณิตศาสตร์
ปีการศึกษา 2550

ลายมือชื่อนักศึกษา ศ. นว
ลายมือชื่ออาจารย์ที่ปรึกษา GR
ลายมือชื่ออาจารย์ที่ปรึกษาร่วม Grigorenko


CHATCHAWAN WATCHARARUANGWIT : DEVELOPMENT OF
A DETERMINISTIC SPECTRAL METHOD FOR SOLVING THE
NONLINEAR BOLTZMANN KINETIC EQUATION. THESIS
ADVISOR : PROF. SERGEY MELESHKO, Ph.D., 77 PP.

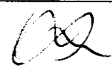
BOLTZMANN EQUATION/MAXWELLIAN MODEL/FOURIER
TRANSFORM/HANKEL TRANSFORM/HEAT TRANSFER PROBLEM

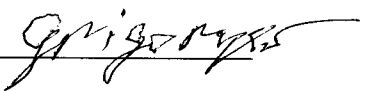
A new deterministic numerical method for solving the kinetic Boltzmann equation of Maxwell molecules with cylindrical symmetry in the velocity space is developed. Using the splitting method with respect to physical processes, the Boltzmann equation is decomposed into the space homogeneous Boltzmann equation and the transport equation. The transport equation is solved by either Lax-Wendroff or upwind schemes. For Maxwell's model, the space homogeneous Boltzmann equation is simplified by Fourier transform with respect to velocity. Because of the cylindrical symmetry in the velocity space, the three-dimensional Fourier transform is equivalent to a one-dimensional Fourier transform and a Hankel transform. An exponential grid in velocity space allows applying an effective FFT algorithm to computing the Hankel transform. The space homogeneous Boltzmann equation in Fourier space is solved by the Runge-Kutta scheme. The new method is applied to solve the heat transfer problem and recondensation problem between parallel plates.

School of Mathematics

Academic Year 2007

Student's Signature 

Advisor's Signature 

Co-advisor's Signature 

ACKNOWLEDGEMENTS

I would like to express my sincere gratitude and deep appreciation to Prof. Dr. Sergey V. Meleshko, my thesis advisor for his support, patient help and offering many useful suggestions. Not only has he guided me throughout the thesis work, but also taken care of my well-being over the years of my study.

I am profoundly grateful to Prof. Dr. Yurii N. Grigoriev, my thesis co-advisor for his collaboration, guidance, supervision and invaluable advice concerning this thesis. I am also deeply indebted to him and his family for their kind assistance throughout my invaluable experience in Russia.

I would like to express my appreciation to Assoc. Prof. Dr. Prapasri Asawakun, Asst. Prof. Dr. Eckart Schulz, Assoc. Prof. Dr. Nikolay Moshkin for being the thesis committee, teaching and helping me during the course of studies at Suranaree University of Technology (SUT).

I would like to thank Asst. Prof. Dr. Jessada Tanthanuch and Mr. Suppiya Siranan for setting up the L^AT_EX format of the thesis and their helpfulness.

I wish to thank the Center for Computing Services and the School of Mathematics at SUT for making available computing facilities throughout this work. I also wish to thank the Institute of Computational Technologies, Siberian Branch of the Russian Academy of Sciences, Novosibirsk, Russia for being my workplace during short term visit.

A special debt of gratitude is expressed to the Development and Promotion of Science and Technology Talents Project and the Royal Golden Jubilee for the scholarship which enabled me to complete my study.

Chatchawan Watchararuangwit

CONTENTS

	Page
ABSTRACT IN THAI	I
ABSTRACT IN ENGLISH	II
ACKNOWLEDGEMENTS	III
CONTENTS	IV
LIST OF TABLES	VII
LIST OF FIGURES	VIII
 CHAPTER	
I INTRODUCTION	1
1.1 The distribution function	3
1.2 The Boltzmann equation	4
1.3 The Macroscopic properties	7
II CONCEPT OF SPECTRAL ANALYSIS IN DISCRETE SPACES	8
2.1 Fourier Transform	8
2.1.1 Continuous Fourier Transform (CFT)	8
2.1.2 Discrete Fourier Transform (DFT)	9
2.1.3 Application of DFT to CFT	9
2.1.4 Application of DFT to discrete convolution	12
2.1.5 Application of DFT to continuous convolution	14
2.2 Hankel Transform	15
2.3 Relationship between Fourier and Hankel transforms	18

CONTENTS (Continued)

	Page
2.4 Fourier Transform of the space homogeneous Boltzmann equation	20
2.5 Fourier Transform of the collision integral for Maxwell molecules. Case of a distribution function with cylindrical symmetry	24
III NUMERICAL SCHEMES FOR PROBLEMS WITH RECT-ANGULAR SPACE GEOMETRY	30
3.1 General formulation of the problems	30
3.2 Dimensionless analysis	31
3.3 Splitting algorithm	32
3.4 Algorithm for heat transfer between parallel plates	33
3.4.1 Grid construction	34
3.4.2 Solving the transport problem in physical space	36
3.4.3 Solving the space homogeneous Boltzmann equation in the Fourier space	39
3.4.4 Relation of two stages of the splitting method	39
3.5 Improvements of the algorithm	41
3.5.1 Conservation laws at the relaxation stage	41
3.5.2 Discrete conservation laws	43
3.5.3 Asymptotic solution of the relaxation problem near zero grid point	44
3.5.4 Numerical procedure	45
IV RESULTS, DISCUSSION AND CONCLUSION	47

CONTENTS (Continued)

	Page
4.1 Qualitative behavior of the solution of problems with rectangular geometry	47
4.1.1 Comparative behavior of hydrodynamic profiles for different types of molecules	47
4.2 Testing the splitting method stages	50
4.2.1 Testing finite-difference schemes for the transport stage . . .	50
4.2.2 Testing the algorithm of the relaxation stage	53
4.3 Heat transfer problem between parallel plates	56
4.4 Recondensation between parallel plates	62
4.5 Conclusion	65
REFERENCES	67
APPENDICES	
APPENDIX A CUBIC SPLINE INTERPOLATION AND QUADRATURE	70
APPENDIX B CALCULATION OF SOME INTEGRALS	74
APPENDIX C INTEGRAL IDENTITY	76
CURRICULUM VITAE	77

LIST OF TABLES

Table		Page
4.1	Comparison between exact and numerical hydrodynamic variables .	52
4.2	Comparison between exact (Maxwell solution) and numerical solution (relative L_∞ -norm of error), $\tau = 0.05$	54
4.3	Comparison between exact (BKW solution) and numerical solution (relative L_∞ -norm of error), $\tau = 0.05$	55
4.4	Mean velocity and heat flux at the stationary solution for $Kn_M = 1$ (Maxwell model).	61

LIST OF FIGURES

Figure	Page
1.1	Flow regimes. 2
2.1	(a). Gaussian function. (b). Exact and numerical Hankel transform of Gaussian function. (c). Absolute error of numerical Hankel transform of Gaussian function. (d). Top-hat function. (e). Exact and numerical Hankel transform of top-hat function. (f). Absolute error of numerical Hankel transform of top-hat function. 19
2.2	Angle between vectors. 25
3.1	Flow between two flat plates. 30
3.2	Realization of the splitting method. 34
3.3	(a) Picture of characteristics. (b) Velocity domains where solution of (3.13) is found. 38
3.4	Connection between physical and Fourier space. 40
4.1	Stencil for asymptotic approximation. 55
4.2	Convergence of the density profiles for $Kn = \frac{1}{2\sqrt{2}}$ 58
4.3	Convergence of the temperature profiles for $Kn = \frac{1}{2\sqrt{2}}$ 58
4.4	Convergence of the density profiles for $Kn = 1.0$ 59
4.5	Convergence of the temperature profiles for $Kn = 1.0$ 59
4.6	Density profiles for different Knudsen number. $Kn_S = 0.01, 0.1, 1;$ $Kn_M = \frac{1}{20\sqrt{2}}, 0.25, \frac{1}{2\sqrt{2}}, 1.$ 60
4.7	Temperature profiles for different Knudsen number. $Kn_S = 0.01,$ $0.1, 1; Kn_M = \frac{1}{20\sqrt{2}}, 0.25, \frac{1}{2\sqrt{2}}, 1.$ 60

LIST OF FIGURES (Continued)

Figure		Page
4.8	Comparison of the shearing of the distribution function	62
4.9	Convergence of the density profiles for $Kn = 0.125$	64
4.10	Convergence of the temperature profiles for $Kn = 0.125$	64

CHAPTER I

INTRODUCTION

The theory of gas dynamics is approached from two perspectives: macroscopic or microscopic. For the macroscopic approach, one considers gas to be a continuum and employs equations such as Navier-Stokes using hydrodynamics variables, i.e., density, velocity, pressure and temperature. The dependent variables in these equations are the macroscopic properties whereas the independent variables are the spatial coordinates and time. This approach works well for gas of a relatively high density. However, for low density or rarefied problems in which the average value of the distance between two subsequent collisions of a molecule (the so-called mean free path, λ) is not negligible in comparison with a length typical of the structure of the flow being considered (e.g., the radius of a pipe or the radius of curvature of the nose of a space shuttle), the continuum approach breaks down. In these cases, one must treat gas microscopically, i.e., consider it to be a set of particles instead of a continuum. Under idealized conditions, if the position, velocity and state of each molecule is known at all times, the gas motion can be determined exactly. However, this is not practical due to the huge number of particles, and mathematical models (using statistical quantities) are used instead. This more general situation can be described by the Boltzmann equation. In this case the only dependent variable is the velocity distribution function (fraction of molecules with certain speeds at a given location and time), but the independent variables are increased to seven (3 velocity components, 3 spatial coordinates and time).

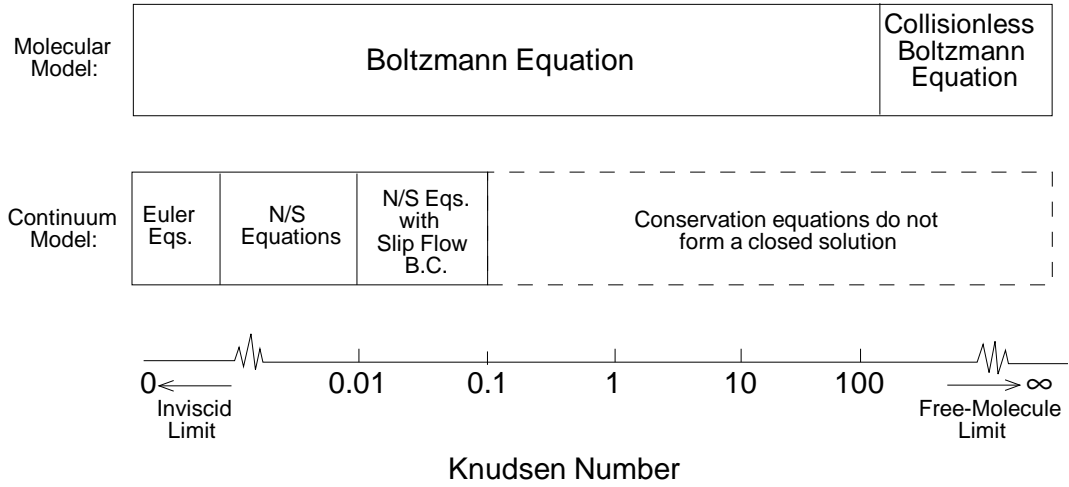


Figure 1.1 Flow regimes.

An important dimensionless parameter, the Knudsen Number (Kn), expresses up to which extent the continuum equations are not valid and the molecular approach is to be used. The Knudsen number is defined as the ratio of the mean free path, to the characteristic dimension, L , i.e.

$$Kn = \frac{\lambda}{L}. \quad (1.1)$$

The Kn domain is often divided into four regimes. For $Kn < 0.01$, continuum regime, the Navier-Stokes equations are applied. For $0.01 < Kn < 0.1$, slip flow regime, Navier-Stokes equations are applied with a slip-flow boundary condition. For $0.1 < Kn < 10$, transition regime, the full Boltzmann equation is used. For $Kn > 10$, free molecular regime, the collisionless Boltzmann equation is applied.

The Boltzmann equation has been applied to many fields, e.g., aerospace research, environmental sciences, aerosol reactors, micromachines and vacuum technology (Kogan, 1969; Cercignani, 1975, 1988, 2000). Unfortunately, the Boltzmann equation, even for the simplest cases, is quite difficult to solve analytically or numerically. The difficulty of computation of a numerical solution is due to

the nonlinearity, to the large number of variables and to the five-fold integral that defines the collision operator. As a consequence, most numerical computations are based on probabilistic Monte Carlo techniques, for example, the direct simulation Monte Carlo method (DSMC) (Bird, 1976) and the modified Monte Carlo method (Nanbu, 1983).

The advantages of probabilistic methods are the following. Computational cost is reduced. The methods do not demand high smoothness of physical boundaries or any artificial boundary in the velocity space. The Monte Carlo methods allow to model easily very complicated potentials of intermolecular interaction. Disadvantages of probabilistic methods are as follows. They have very slow convergence, relatively low precision and are unsuitable for modeling high energy tails of distribution functions. The last is of interest for the modeling of threshold kinetic processes.

In this research, we develop a new direct regular numerical method for solving heat transfer and recondensation problems which are described by the Boltzmann equation.

1.1 The distribution function

A gas flow would be completely described, in a classical sense, by listing the position, velocity and internal state of every molecule at a particular instant. For a system composed of N molecules, at any instant, it is convenient to introduce the so-called phase space, i.e., a $6N$ dimensional space, formed by molecular velocities \mathbf{v} and the space coordinate \mathbf{x} . In this space the state of the system is represented by a point whose coordinates are the $6N$ values of the components of the position vectors and velocities of the N particles. Since the number of molecules of a real gas is so large that such a description is unthinkable, we must resort to a statistical

descriptions in terms of probability distributions. Let us introduce a distribution function

$$f = f(\mathbf{x}, \mathbf{v}, t), \quad f : \mathbb{R}^3 \times \mathbb{R}^3 \times \mathbb{R}^+ \longrightarrow \mathbb{R}^+, \quad (1.2)$$

which gives the distribution of probability in phase space, more precisely

$$f(\mathbf{x}, \mathbf{v}, t)d\mathbf{x}d\mathbf{v} \quad (1.3)$$

gives the expected number of molecules in the element volume $d\mathbf{x}d\mathbf{v}$ centered at the phase space point (\mathbf{x}, \mathbf{v}) , at time t .

1.2 The Boltzmann equation

The Boltzmann equation is an integro-differential equation that describes the evolution of rarefied gas in terms of a molecular distribution function. The derivation of the Boltzmann equation is based on the following assumptions (Kogan, 1969; Cercignani, 1975):

- Gas particles move freely in the space. The collisions have instant in time and local in space character. During the collisions the conservation of momentum and energy hold according to the laws of classical mechanics.
- Collisions involving more than two particles are negligible.
- Collisions between pairs of particles are uncorrelated (molecular chaos hypothesis).

Without external forces, the Boltzmann equation for monatomic gas can be written as (Kogan, 1969; Cercignani, 1975)

$$\frac{\partial f}{\partial t} + \mathbf{v} \cdot \nabla_{\mathbf{x}} f = Q(f, f), \quad \mathbf{x}, \mathbf{v} \in \mathbb{R}^3, \quad (1.4)$$

where $f = f(\mathbf{x}, \mathbf{v}, t)$ is a distribution function describing time evolution of the distribution of probability of particles which move with velocity \mathbf{v} in position \mathbf{x} at time $t > 0$. The theory of existence and uniqueness of a local solution of the Boltzmann equation in various settings can be found in (Cercignani, 1975, 1988). The term $Q(f, f)$ is called the collision operator and defined by

$$Q(f, f)(\mathbf{x}, \mathbf{v}, t) = \int_{\mathbb{R}^3} \int_{S^2} B(|\mathbf{v} - \mathbf{v}_1|, \theta) [f(\mathbf{x}, \mathbf{v}', t) f(\mathbf{x}, \mathbf{v}_1', t) - f(\mathbf{x}, \mathbf{v}, t) f(\mathbf{x}, \mathbf{v}_1, t)] d\mathbf{n} d\mathbf{v}_1, \quad (1.5)$$

where \mathbf{v}' and \mathbf{v}_1' are the velocities after a collision of two particles which had velocities \mathbf{v} and \mathbf{v}_1 before the encounter. The deflection angle θ is the angle between $\mathbf{v} - \mathbf{v}_1$ and $\mathbf{v}' - \mathbf{v}_1'$. The collisional velocities satisfy microscopic momentum and energy conservation,

$$\mathbf{v}' + \mathbf{v}_1' = \mathbf{v} + \mathbf{v}_1, \quad |\mathbf{v}'|^2 + |\mathbf{v}_1'|^2 = |\mathbf{v}|^2 + |\mathbf{v}_1|^2. \quad (1.6)$$

The postcollision velocities can be obtained by solving algebraic equations (1.6) and are parameterized by

$$\mathbf{v}' = \frac{1}{2}(\mathbf{v} + \mathbf{v}_1 + |\mathbf{v} - \mathbf{v}_1| \mathbf{n}), \quad \mathbf{v}_1' = \frac{1}{2}(\mathbf{v} + \mathbf{v}_1 - |\mathbf{v} - \mathbf{v}_1| \mathbf{n}),$$

where \mathbf{n} is a unit vector varying on the sphere S^2 ,

$$S^2 = \{\mathbf{n} \in \mathbb{R}^3, \quad |\mathbf{n}| = 1\}.$$

The scattering function B has the form

$$B(|\mathbf{v} - \mathbf{v}_1|, \theta) = |\mathbf{v} - \mathbf{v}_1| \sigma(|\mathbf{v} - \mathbf{v}_1|, \cos(\theta)) \quad (1.7)$$

where $\cos(\theta) = \frac{(\mathbf{v} - \mathbf{v}_1) \cdot \mathbf{n}}{|\mathbf{v} - \mathbf{v}_1|}$. The function $\sigma : \mathbb{R}^+ \times [-1, 1] \rightarrow \mathbb{R}^+$ is the differential cross-section and θ is the scattering angle. The scattering function B characterizes the details of the binary interactions, depends on the physical properties of gas.

Some types of collision scattering function frequently considered in the Boltzmann equation are the following

1. Inverse power potentials. In this model, the particle interaction is described by potentials of order m and the scattering function acquires the form

$$B(|\mathbf{v} - \mathbf{v}_1|, \theta) = b_\lambda(\cos(\theta))|\mathbf{v} - \mathbf{v}_1|^\lambda, \quad \lambda = 1 - \frac{4}{m}, \quad m > 1. \quad (1.8)$$

$b_\lambda(\cos(\theta))$ is a continuous function on the semi-closed interval $[-1, 1)$ and has a non-integrable singularity at $\cos(\theta) = 1$ of order

$$b_\lambda(\cos(\theta)) = O((1 - \cos(\theta))^{(\lambda-5)/4}), \quad -3 < \lambda \leq 1. \quad (1.9)$$

The condition (1.9) implies that the function $b_\lambda(\cos(\theta))(1 - \cos(\theta))$ is integrable on the interval $[-1, 1]$. For $0 < \lambda \leq 1$ the potential is called hard, for $-3 < \lambda < 0$ the potential is called soft. The special case $\lambda = 0$ corresponds to the Maxwell molecules with

$$B(|\mathbf{v} - \mathbf{v}_1|, \theta) = b_0(\cos(\theta)). \quad (1.10)$$

The collision scattering function $B(|\mathbf{v} - \mathbf{v}_1|, \theta)$ here does not depend on the relative speed $|\mathbf{v} - \mathbf{v}_1|$.

2. The Grad's cutoff assumption supposes the function b_λ to be integrable, i.e.

$$C_\lambda = 2\pi \int_{-1}^1 b_\lambda(\cos(\theta))d(\cos(\theta)) < \infty. \quad (1.11)$$

3. In many practical applications, the interaction is considered to be independent of the scattering angle, as described by the Variable Hard Spheres model (VHS)

$$B(|\mathbf{v} - \mathbf{v}_1|, \theta) = \frac{C_\lambda}{4\pi} |\mathbf{v} - \mathbf{v}_1|^\lambda, \quad -3 < \lambda \leq 1. \quad (1.12)$$

The model includes as particular cases the hard spheres model for $\lambda = 1$

$$B(|\mathbf{v} - \mathbf{v}_1|, \theta) = \frac{d^2}{4} |\mathbf{v} - \mathbf{v}_1|, \quad (1.13)$$

where d denotes the diameter of the particles and the isotropic Maxwell molecules for $\lambda = 0$.

The Boltzmann collision operator has the following fundamental properties of conserving mass, momentum, and energy:

$$\int_{\mathbb{R}^3} Q(f, f) d\mathbf{v} = 0, \quad (1.14)$$

$$\int_{\mathbb{R}^3} \mathbf{v} Q(f, f) d\mathbf{v} = 0, \quad (1.15)$$

$$\int_{\mathbb{R}^3} |\mathbf{v}|^2 Q(f, f) d\mathbf{v} = 0, \quad (1.16)$$

and satisfies the well-known Boltzmann H -theorem

$$\int_{\mathbb{R}^3} Q(f, f) \log(f) d\mathbf{v} \leq 0. \quad (1.17)$$

1.3 The Macroscopic properties

When the distribution function f of the gas is known, all the macroscopic properties of the gas of concern in gas dynamics can be obtained by finding the moments of f . By finding the moments of f we mean multiplying f by a certain function of molecular velocity and taking integral over the entire velocity space. Let $n(\mathbf{x}, t)$, $\mathbf{u}(\mathbf{x}, t)$ and $T(\mathbf{x}, t)$ be the density, mean velocity and temperature of the gas respectively, then

$$n(\mathbf{x}, t) = \int_{\mathbb{R}^3} f(\mathbf{v}) d\mathbf{v}, \quad (1.18)$$

$$\mathbf{u}(\mathbf{x}, t) = \frac{1}{n(\mathbf{x}, t)} \int_{\mathbb{R}^3} \mathbf{v} f(\mathbf{v}) d\mathbf{v}, \quad (1.19)$$

$$T(\mathbf{x}, t) = \frac{1}{3n(\mathbf{x}, t)R} \int_{\mathbb{R}^3} |\mathbf{v} - \mathbf{u}|^2 f(\mathbf{v}) d\mathbf{v}, \quad (1.20)$$

where R is a gas constant.

CHAPTER II

CONCEPT OF SPECTRAL ANALYSIS IN DISCRETE SPACES

The transform method is an essential tool for scientists. The basic aim of the transform method is to transform a given problem into one that is easier to solve. In this chapter, we will introduce Fourier and Hankel transforms which are the important tool for the proposed numerical method of solving the Boltzmann equation.

2.1 Fourier Transform

2.1.1 Continuous Fourier Transform (CFT)

Let $f(x) : \mathbb{R} \rightarrow \mathbb{R}$ satisfy the following conditions:

1. $f(x)$ and $f'(x)$ are piecewise continuous in every finite interval.

2.
$$\int_{-\infty}^{\infty} |f(x)| dx < \infty.$$

Fourier's integral theorem states that (Snedon, 1972)

$$f(x) = \int_{-\infty}^{\infty} \left(\int_{-\infty}^{\infty} f(x) e^{-i2\pi kx} dx \right) e^{i2\pi kx} dk, \quad (2.1)$$

where $f(x)$ on the left hand side is to be understood as $\frac{f(x^+) + f(x^-)}{2}$. The function

$$F(k) := \int_{-\infty}^{\infty} f(x) e^{-i2\pi kx} dx \quad (2.2)$$

is called the Fourier transform of $f(x)$.

The Fourier transform pairs in n -dimensions can be defined for $\mathbf{k}, \mathbf{x} \in \mathbb{R}^n$ by

$$F(\mathbf{k}) = \int_{\mathbb{R}^n} e^{-i2\pi\mathbf{k}\cdot\mathbf{x}} f(\mathbf{x}) d\mathbf{x} \quad (2.3)$$

$$f(\mathbf{x}) = \int_{\mathbb{R}^n} e^{i2\pi\mathbf{k}\cdot\mathbf{x}} F(\mathbf{k}) d\mathbf{k} \quad (2.4)$$

where $\mathbf{k} \cdot \mathbf{x} = \sum_{i=1}^n k_i x_i$.

2.1.2 Discrete Fourier Transform (DFT)

Let $\{c_k\}_{k=0}^{N-1}$ be a sequence of complex numbers. Then the Discrete Fourier Transform (DFT) of $\{c_k\}_{k=0}^{N-1}$ denoted by $\{\tilde{c}_n\}_{n=0}^{N-1}$ is defined as

$$\tilde{c}_n = \sum_{k=0}^{N-1} c_k e^{\frac{-2\pi i k n}{N}}, \quad (2.5)$$

and the original sequence c_k can be reconstructed by

$$c_k = \frac{1}{N} \sum_{n=0}^{N-1} \tilde{c}_n e^{\frac{2\pi i k n}{N}}. \quad (2.6)$$

The discrete Fourier transform has been widely used to estimate values for the continuous Fourier transform. However, the straightforward calculation of discrete Fourier transform leads to an algorithm with quadratic complexity in N ($O(N^2)$) which needs much computation effort. Fortunately, one exploits some symmetries of the complex exponentials and derives a recursive formulation that leads to a fast algorithm which is called **Fast Fourier Transform (FFT)** (Cooley and Turkey, 1965). The complexity in calculation is reduced to $O(N \log_2 N)$. Therefore, the FFT is an efficient numerical algorithm.

2.1.3 Application of DFT to CFT

First, let us assume that $f(x) \sim 0$ outside the interval $[0, T]$. Thus we have

$$F(u) \approx \int_0^T f(x) e^{-i2\pi u x} dx. \quad (2.7)$$

The integral is then approximated by a uniform, left-endpoint sum

$$\int_0^T f(x)e^{-i2\pi ux} dx \approx \frac{T}{N} \sum_{j=0}^{N-1} f\left(j\frac{T}{N}\right)e^{-i2\pi ujT/N}.$$

Thus,

$$F(u) \approx \frac{T}{N} \sum_{j=0}^{N-1} f\left(j\frac{T}{N}\right)e^{-i2\pi ujT/N}. \quad (2.8)$$

To convert the right side of (2.8) into a DFT we replace u by $\frac{k}{T}$ for $k \in I$,

$$F\left(\frac{k}{T}\right) \approx \frac{T}{N} \sum_{j=0}^{N-1} f\left(j\frac{T}{N}\right)e^{-i2\pi kj/N}. \quad (2.9)$$

The right side of (2.9) is equal to $\frac{T}{N}$ times the N -point DFT of the sequence

$$\left\{ f\left(j\frac{T}{N}\right) \right\}_{j=0}^{N-1}. \quad (2.10)$$

Let us denote by c_k the N -point DFT of (2.10). By periodicity, we can define c_{-k} by

$$c_{-k} = c_{N-k}$$

and, hence

$$\begin{aligned} F\left(\frac{k}{T}\right) &\approx \frac{T}{N}c_k & \text{for } k = 0, 1, \dots, \frac{N}{2} - 1 \\ F\left(\frac{-k}{T}\right) &\approx \frac{T}{N}c_{N-k} & \text{for } k = 1, 2, \dots, \frac{N}{2}. \end{aligned} \quad (2.11)$$

Consider a more general case, which would be to assume that $f(x) \sim 0$ outside the interval $[-\frac{T}{2}, \frac{T}{2}]$ for some large T . Then we will have

$$F(k) \approx \int_{-\frac{T}{2}}^{\frac{T}{2}} f(x)e^{-i2\pi kx} dx \quad (2.12)$$

We have

$$F\left(\frac{k}{T}\right) \approx \int_{-\frac{T}{2}}^{\frac{T}{2}} f(x)e^{-i2\pi kx/T} dx. \quad (2.13)$$

Splitting the integral in (2.13) into two integrals, we can change variables so that we are integrating over $[0, T]$

$$\int_{-\frac{T}{2}}^{\frac{T}{2}} f(x)e^{-i2\pi kx/T} dx = \int_{-\frac{T}{2}}^0 f(x)e^{-i2\pi kx/T} dx + \int_0^{\frac{T}{2}} f(x)e^{-i2\pi kx/T} dx. \quad (2.14)$$

Substituting $t = x + T$ into the first integral on the right side of (2.14) yields

$$\begin{aligned} \int_{-\frac{T}{2}}^{\frac{T}{2}} f(x)e^{-i2\pi kx/T} dx &= \int_{\frac{T}{2}}^T f(t-T)e^{-i2\pi kt/T} dt + \int_0^{\frac{T}{2}} f(x)e^{-i2\pi kx/T} dx \\ &= \int_{\frac{T}{2}}^T f(x-T)e^{-i2\pi kx/T} dx + \int_0^{\frac{T}{2}} f(x)e^{-i2\pi kx/T} dx. \end{aligned} \quad (2.15)$$

Thus, if we define g by

$$g(x) = \begin{cases} f(x), & 0 \leq x < \frac{T}{2} \\ \frac{f(\frac{T}{2})+f(-\frac{T}{2})}{2}, & x = \frac{T}{2} \\ f(x-T), & \frac{T}{2} < x \leq T. \end{cases} \quad (2.16)$$

We have

$$\int_{-\frac{T}{2}}^{\frac{T}{2}} f(x)e^{-i2\pi kx/T} dx = \int_0^T g(x)e^{-i2\pi kx/T} dx. \quad (2.17)$$

Using (2.17) we have from (2.13) that

$$F\left(\frac{k}{T}\right) \approx \int_0^T g(x)e^{-i2\pi kx/T} dx. \quad (2.18)$$

Then, as we did above for (2.7), we can approximate the right side of (2.18) by $\frac{T}{N}$ times an N -point DFT

$$F\left(\frac{k}{T}\right) \approx \frac{T}{N} \sum_{j=0}^{N-1} g\left(j\frac{T}{N}\right)e^{-i2\pi jk/N}. \quad (2.19)$$

We will show that there is another formula for approximating CFT with DFT for this general case. We approximate the integral in (2.13) by the uniform, left-endpoint sum

$$F\left(\frac{k}{T}\right) \approx \frac{T}{N} \sum_{j=-\frac{N}{2}}^{\frac{N}{2}-1} f\left(j\frac{T}{N}\right)e^{-i2\pi jk/N}, \quad k = -\frac{N}{2}, \dots, \frac{N}{2} - 1. \quad (2.20)$$

In order to use FFT algorithm for summation on the right side of (2.20), we replace j by $j - \frac{N}{2}$ and k by $k - \frac{N}{2}$. Then (2.20) becomes

$$F\left(\frac{k - \frac{N}{2}}{T}\right) \approx \frac{T}{N} \sum_{j=0}^{N-1} f\left(\frac{(j - \frac{N}{2})T}{N}\right) e^{-i2\pi(k - \frac{N}{2})(j - \frac{N}{2})/N}, \quad k = 0, \dots, N-1. \quad (2.21)$$

If N is even,

$$e^{-i2\pi(k-\frac{N}{2})(j-\frac{N}{2})/N} = (-1)^k(-1)^j e^{-i2\pi jk/N},$$

we get

$$F\left(\frac{k-\frac{N}{2}}{T}\right) \approx (-1)^k \frac{T}{N} \sum_{j=0}^{N-1} (-1)^j f\left(\frac{(j-\frac{N}{2})T}{N}\right) e^{-i2\pi jk/N}, \quad k = 0, \dots, N-1. \quad (2.22)$$

The analogy can be made for higher dimension, that is, if

$$f(x_1, x_2, \dots, x_n) \approx 0 \quad \text{for } |x_i| > \frac{T_i}{2}, \quad i = 1, 2, \dots, n$$

then

$$\begin{aligned} & F\left(\frac{k_1-\frac{N_1}{2}}{T_1}, \frac{k_2-\frac{N_2}{2}}{T_2}, \dots, \frac{k_n-\frac{N_n}{2}}{T_n}\right) \\ & \approx (-1)^{\sum_{i=1}^n k_i} \left(\prod_{i=1}^n \frac{T_i}{N_i} \right) \sum_{j_n=0}^{N_n-1} \sum_{j_{n-1}=0}^{N_{n-1}-1} \dots \sum_{j_1=0}^{N_1-1} (-1)^{\sum_{i=1}^n j_i} \\ & \quad f\left(\frac{(j_1-\frac{N_1}{2})T_1}{N_1}, \frac{(j_2-\frac{N_2}{2})T_2}{N_2}, \dots, \frac{(j_n-\frac{N_n}{2})T_n}{N_n}\right) e^{-i2\pi \sum_{i=1}^n \frac{j_i k_i}{N_i}} \end{aligned} \quad (2.23)$$

for $k_i = 0, \dots, N_i - 1$.

2.1.4 Application of DFT to discrete convolution

Definition 2.1 (circular convolution). Let $\{x_n\}$ and $\{y_n\}$ be two sequences of complex numbers, each having period N . The circular convolution of $\{x_n\}$ and $\{y_n\}$ is the sequence $\{(x \circledast y)_n\}$ defined by

$$(x \circledast y)_n = \sum_{i=0}^{N-1} x_i y_{n-i}. \quad (2.24)$$

Theorem 2.1 (discrete convolution theorem). *If $\{x_n\}$ and $\{y_n\}$ are sequences of period N with DFTs $\{X_n\}$ and $\{Y_n\}$, respectively, then the DFT of $\{(x \circledast y)_n\}$ is $\{X_n Y_n\}$.*

The direct evaluation of the convolution summation (2.24) requires $O(N^2)$ operations. The discrete convolution theorem shows how efficiently to compute the circular convolution. From discrete convolution theorem, we have

$$\{(x \otimes y)_n\} = DFT^{-1} [DFT\{x_n\} \times DFT\{y_n\}]. \quad (2.25)$$

By taking the advantage of the FFT, the complexity of calculation of circular convolution is reduced to $O(N \log_2 N)$.

Definition 2.2 (linear convolution). Let $\{x_n\}$ and $\{y_n\}$ be two summable sequences of complex numbers. The linear convolution of $\{x_n\}$ and $\{y_n\}$ is the sequence $\{(x * y)_n\}$ defined by

$$(x * y)_n = \sum_{i=-\infty}^{\infty} x_i y_{n-i}. \quad (2.26)$$

Note that here finite sequences are extended to infinite sequences by padding with zeros.

The linear convolution is often encountered in applications, for instance, the discrete version of the convolution integral is used in fast Hankel transform algorithm (Section 2.2). However, the computational advantage of using the FFT is potentially a very attractive method of achieving convolution. Fortunately, we can apply the circular convolution algorithm to linear convolution by padding with sufficient zeros. More precisely, suppose we have two sequences $\{x_n\}_{n=0}^{M_1-1}$ and $\{y_n\}_{n=0}^{M_2-1}$. Let us choose $N = 2^k$ for some $k \in \mathbb{N}$ such that $N \geq M_1 + M_2 - 1$. Define $\{\tilde{x}_n\}_{n=0}^{M_1-1}$ and $\{\tilde{y}_n\}_{n=0}^{M_2-1}$ by

$$\begin{aligned} \tilde{x}_n &= x_n & \text{for } n &= 0, 1, \dots, M_1 - 1 \\ \tilde{x}_n &= 0 & \text{for } n &= M_1, M_1 + 1, \dots, N - 1 \\ \tilde{y}_n &= y_n & \text{for } n &= 0, 1, \dots, M_2 - 1 \\ \tilde{y}_n &= 0 & \text{for } n &= M_2, M_2 + 1, \dots, N - 1, \end{aligned}$$

then

$$(\tilde{x} \circledast \tilde{y})_n = (x * y)_n.$$

Although the lengths of these two sequences are not necessary equal, they are regarded as identical sequences since the first $M_1 + M_2 - 1$ terms are the same, except for the additional zeros added at the end of $\tilde{x} \circledast \tilde{y}$.

2.1.5 Application of DFT to continuous convolution

The important application of circular convolution is to approximate the continuous convolution. Consider convolution of functions f and g

$$(f * g)(x) = \int_{-\infty}^{\infty} f(t)g(x - t)dt. \quad (2.27)$$

There are three cases to be considered.

Case 1. $\text{supp}(f) \subset [0, T_1]$ and $\text{supp}(g) \subset [0, T_2]$.

To compute the continuous convolution numerically, we sample the functions f and g over their support with the sample interval h . Let M_1 and M_2 be the number of samples taken from f and g , respectively. Then

$$(f * g)(kh) \approx h \sum_{i=0}^{M_1+M_2-1} f(ih)g((k-i)h), \quad k = 0, 1, \dots, N - 1. \quad (2.28)$$

Equation (2.28) is simply the continuous convolution integral evaluated by rectangular integration. Then we can apply the circular convolution algorithm to the right hand side of (2.28) by choosing $N = 2^m \geq M_1 + M_2 - 1$ for some $m \in \mathbb{N}$.

Case 2. $\text{supp}(f) \subset [0, T_1]$ and $\text{supp}(g) = \mathbb{R}$.

Since the computer can process only a finite set of data, we decompose the support of the function g into smaller sections and compute the convolution

as many smaller convolutions, leading to the concept of *sectioning* (Brigham, 1974). The sectioned convolution is computed until the interval of interest for the convolution is obtained. We first take M samples from f and form the sampled sequence f_n . Then choose $N = 2^m > M$ for some $m \in \mathbb{N}$ and form the sampled sequence g_n . Then extend the length of the sequence f_n to N by zero padding. Now we can apply the circular algorithm (2.25) to perform convolution of sequences f_n and g_n . Note that the first $M - 1$ points of the result are incorrect because of the *end effect* (Brigham, 1974). The remaining sectioned convolution can be done similarly by shifting the considered section to the origin. The sectioned convolution results are then shifted back to the proper position.

Case 3. $\text{supp}(f)$ or $\text{supp}(g)$ is an arbitrary finite interval.

In this case, we shift the function with finite support to make its support begin at the origin. Then either case 1 or case 2 can be applied. Afterward, the result must be shifted back to the proper position.

2.2 Hankel Transform

Let $f(r)$ be a function defined for $r \geq 0$. The ν^{th} order Hankel Transform of $f(r)$ is defined as

$$g(k) = 2\pi \int_0^\infty r f(r) J_\nu(2\pi kr) dr, \quad (2.29)$$

where $J_\nu(x)$ is the Bessel function of the first kind and of order ν . If $\nu > -\frac{1}{2}$, then the inversion formula is

$$f(r) = 2\pi \int_0^\infty k g(k) J_\nu(2\pi kr) dk. \quad (2.30)$$

Sufficient but not necessary conditions for the validity of (2.29) and (2.30) are (Poularikas, 1996)

1. $f(r) = O(r^{-s})$, where $s > \frac{3}{2}$.
2. $f'(r)$ is piecewise continuous over each bounded subinterval of $[0, \infty)$.
3. $f(r)$ is defined as $\frac{f(r^+) + f(r^-)}{2}$.

As for computing the Hankel transform numerically, Siegmann was the first to propose an algorithm that applies the computational efficiency of the FFT (Siegmann, 1977). By an exponential transform of the independent variables, the Hankel transform becomes a one dimensional convolution type integral which is then evaluated by the use of the FFT. This algorithm involves the Fourier transform three times.

In this thesis, we use the exponential transform and some special splitting of the integrand in (2.29) to derive a fast algorithm for computing the Hankel transform numerically. This algorithm involves a two time Fourier transform and the integral of a Bessel function which can be integrated analytically. More precisely, considering an exponential transform,

$$k = k_0 e^x, \quad r = r_0 e^{-y}, \quad (2.31)$$

equation (2.29) is transformed to

$$\begin{aligned} g(k_0 e^x) &= 2\pi \int_{-\infty}^{\infty} r_0^2 e^{-2y} f(r_0 e^{-y}) J_0(2\pi k_0 r_0 e^{x-y}) dy \\ &= 2\pi e^{-x} \int_{-\infty}^{\infty} r_0^2 e^{-y} f(r_0 e^{-y}) e^{x-y} J_0(2\pi k_0 r_0 e^{x-y}) dy. \end{aligned} \quad (2.32)$$

Let

$$\tilde{g}(x) = g(k_0 e^x), \quad p(y) = r_0^2 e^{-y} f(r_0 e^{-y}), \quad q(y) = e^y J_0(2\pi k_0 r_0 e^y),$$

then equation (2.32) becomes

$$\tilde{g}(x) = 2\pi e^{-x} \int_{-\infty}^{\infty} p(y) q(x-y) dy. \quad (2.33)$$

Equation (2.33) is a convolution of functions $p(y)$ and $q(y)$. By using the Fourier convolution theorem, if

$$\Phi(t) = \int_{-\infty}^{\infty} e^{-i2\pi ty} p(y) dy \quad (2.34)$$

and

$$M(t) = \int_{-\infty}^{\infty} e^{-i2\pi ty} q(y) dy \quad (2.35)$$

then the Hankel transform on the exponential grid can be written as

$$\tilde{g}(x) = 2\pi e^{-x} \int_{-\infty}^{\infty} e^{i2\pi xt} \Phi(t) M(t) dt. \quad (2.36)$$

By substitution of $q(y) = e^y J_0(2\pi k_0 r_0 e^y)$ and letting $r = e^y$, equation (2.35) becomes

$$M(t) = \int_0^{\infty} r^{-i2\pi t} J_0(2\pi k_0 r_0 r) dr. \quad (2.37)$$

The integral on the right hand side of (2.37) can be integrated analytically (Luke, 1962) so that

$$M(t) = \frac{1}{2} (\pi k_0 r_0)^{-1+i2\pi t} \frac{\Gamma(\frac{1-i2\pi t}{2})}{\Gamma(\frac{1+i2\pi t}{2})} \quad (2.38)$$

where $\Gamma(x)$ is the gamma function. The values of the function $M(t)$ are computed and stored in a table to be used for the subsequent Hankel transforms, in order to save computational time.

To compute the Hankel transform numerically, the parameters r_0 and k_0 have to be chosen according to certain criteria. Let us assume that the truncated intervals (r_{min}, r_{max}) and (k_{min}, k_{max}) contain most of the function f (resp. g) in the r -domain (resp. k -domain). Then we set

$$r_0 = r_{max}, \quad r_{min} = r_0 e^{-(N-1)h}, \quad k_0 = k_{min}, \quad k_{max} = k_0 e^{(N-1)h}$$

where N is the number of samples and $h = \frac{1}{(N-1)} \ln(\frac{r_{max}}{r_{min}})$.

The algorithm was tested with the Gaussian function

$$f_1(r) = e^{-\pi r^2},$$

and the top-hat function

$$f_2(r) = \begin{cases} 1, & 0 \leq r \leq 2, \\ 0, & \text{otherwise,} \end{cases}$$

which have exact Hankel transform (Poularikas, 1996)

$$g_1(k) = e^{-\pi k^2},$$

and

$$g_2(k) = \frac{2J_1(4\pi k)}{k},$$

respectively. The results of calculations are shown in Figure 2.1. The parameters for computing the Hankel transform of the Gaussian function are $N = 256, r_0 = 4, k_0 = 0.001$ and $h = 0.0325$. For the top-hat function, the parameters are $N = 256, r_0 = 2, k_0 = 0.01$ and $h = 0.0208$. The comparison between the exact and numerical Hankel transforms of the Gaussian and top-hat functions are shown in Figure 2.1(b) and 2.1(e). We can not see the difference at this scale since the absolute error is small. In order to compare the numerical result with the exact one, the relative L_∞ -norm of error which is defined as $\frac{\max_{0 \leq i < N} |f_i^{(numerical)} - f_i^{(exact)}|}{\max_{0 \leq i < N} |f_i^{(exact)}|}$ is used. The relative L_∞ -norm of error for the Gaussian function and top-hat functions are 1.1×10^{-9} and 2.8×10^{-4} respectively.

2.3 Relationship between Fourier and Hankel transforms

The two-dimensional problem often exhibits circular symmetry for natural reasons. In this case, it may be expected that a simplification will result since one radial variable will suffice in place of two independent rectangular coordinates. Let us assume that

$$f(x, y) = g(r), \quad \text{where } r^2 = x^2 + y^2.$$

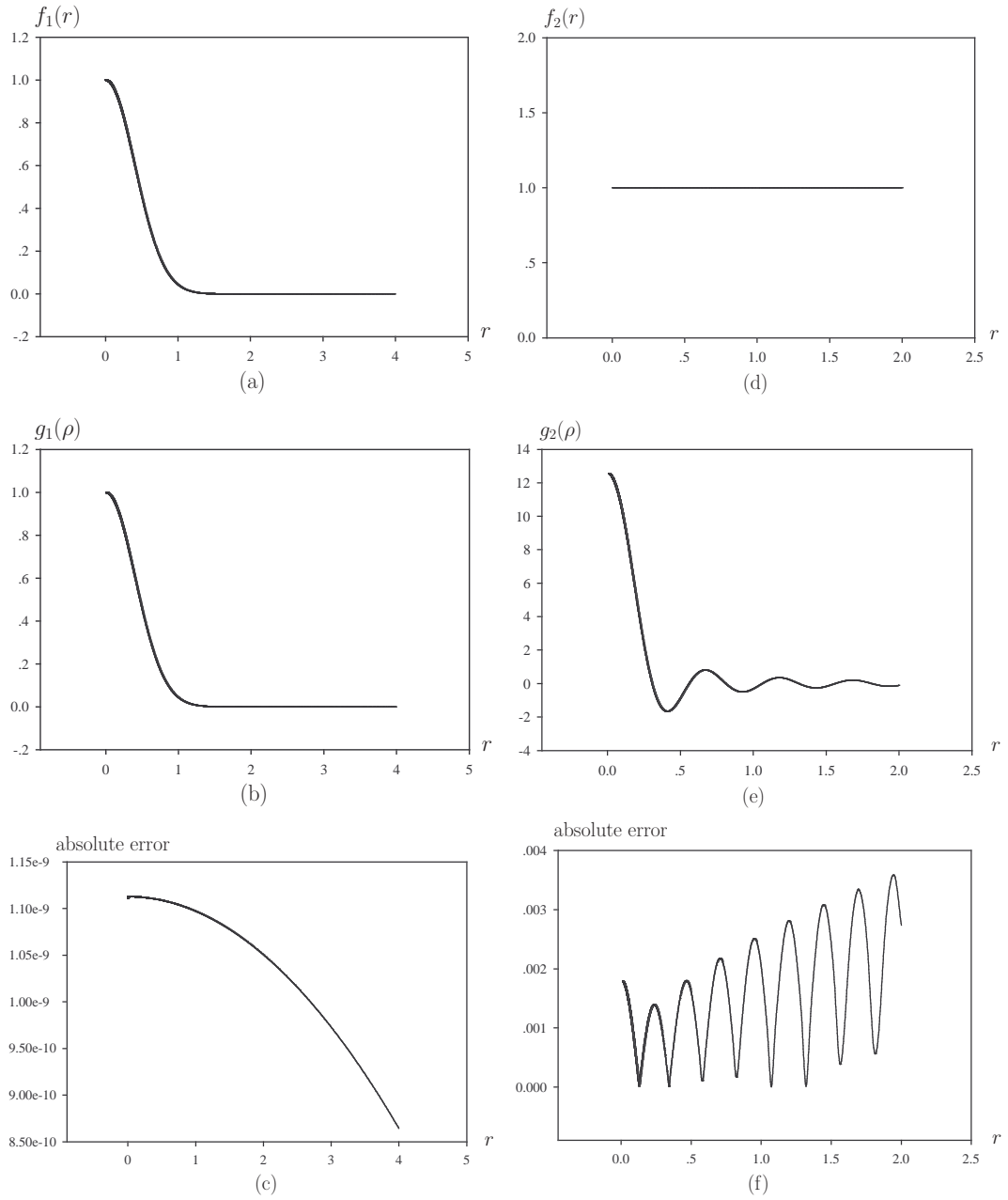


Figure 2.1 (a). Gaussian function. (b). Exact and numerical Hankel transform of Gaussian function. (c). Absolute error of numerical Hankel transform of Gaussian function. (d). Top-hat function. (e). Exact and numerical Hankel transform of top-hat function. (f). Absolute error of numerical Hankel transform of top-hat function.

In terms of the polar coordinates

$$\begin{aligned}x &= r \cos \theta, & y &= r \sin \theta \\u &= \rho \cos \varphi, & v &= \rho \sin \varphi.\end{aligned}$$

The two-dimensional Fourier transform

$$F(u, v) = \int_{-\infty}^{\infty} \int_{-\infty}^{\infty} e^{-i2\pi(ux+vy)} f(x, y) dx dy \quad (2.39)$$

becomes

$$\begin{aligned}F(\rho \cos \varphi, \rho \sin \varphi) &= \int_0^{\infty} \int_0^{2\pi} e^{-i2\pi\rho r \cos(\theta-\varphi)} r g(r) d\theta dr \\&= 2\pi \int_0^{\infty} r g(r) J_0(2\pi\rho r) dr\end{aligned} \quad (2.40)$$

where $J_0(x)$ is the Bessel function of order zero and we have used the identity

$$J_0(x) = \frac{1}{2\pi} \int_0^{2\pi} e^{-ix \cos(\theta)} d\theta. \quad (2.41)$$

Let $G(\rho)$ be the Hankel transform of order zero of $g(r)$, then equation (2.40) implies that

$$G(\rho) = F(\rho \cos \varphi, \rho \sin \varphi) = F(u, v), \quad (2.42)$$

where we have the relation $\rho^2 = u^2 + v^2$.

2.4 Fourier Transform of the space homogeneous Boltzmann equation

Consider the space homogeneous Boltzmann equation

$$\begin{aligned}\frac{\partial f}{\partial t}(\mathbf{x}, \mathbf{v}, t) &= Q(f, f)(\mathbf{x}, \mathbf{v}, t), \\f(\mathbf{x}, \mathbf{v}, 0) &= f_0(\mathbf{x}, \mathbf{v}).\end{aligned} \quad (2.43)$$

The Fourier transform on the velocity space $\varphi(\mathbf{x}, \mathbf{k}, t)$ of the distribution function $f(\mathbf{x}, \mathbf{v}, t)$ is defined as

$$\varphi(\mathbf{x}, \mathbf{k}, t) = \int_{R^3} e^{-i2\pi(\mathbf{v}\cdot\mathbf{k})} f(\mathbf{x}, \mathbf{v}, t) d\mathbf{v}. \quad (2.44)$$

Since the variables \mathbf{x} and t are not invoked when taking Fourier transform on velocity space, for the sake of simplicity, we will write $f(\mathbf{v})$ instead of $f(\mathbf{x}, \mathbf{v}, t)$. More generally, consider an integral of the collision operator multiplied with some function $\phi(\mathbf{v})$,

$$\begin{aligned} J &= \int_{R^3} \phi(\mathbf{v}) Q(f, f)(\mathbf{v}) d\mathbf{v} \\ &= \int_{R^3} \int_{R^3} \int_{S^2} \phi(\mathbf{v}) B(|\mathbf{v} - \mathbf{v}_1|, \theta) [f(\mathbf{v}') f(\mathbf{v}'_1) - f(\mathbf{v}) f(\mathbf{v}_1)] d\mathbf{n} d\mathbf{v}_1 d\mathbf{v}. \end{aligned} \quad (2.45)$$

By interchanging the dummy variables \mathbf{v}, \mathbf{v}_1 and $\mathbf{v}', \mathbf{v}'_1$, equation (2.45) becomes

$$J = \int_{R^3} \int_{R^3} \int_{S^2} \phi(\mathbf{v}') B(|\mathbf{v}' - \mathbf{v}'_1|, \theta) [f(\mathbf{v}) f(\mathbf{v}_1) - f(\mathbf{v}') f(\mathbf{v}'_1)] d\mathbf{n} d\mathbf{v}'_1 d\mathbf{v}'. \quad (2.46)$$

Using equivalent forms of postcollision velocities (Cercignani, 1975, 1988, 2000),

$$\mathbf{v}' = \mathbf{v} - ((\mathbf{v} - \mathbf{v}_1) \cdot \mathbf{n})\mathbf{n}, \quad \mathbf{v}'_1 = \mathbf{v}_1 + ((\mathbf{v} - \mathbf{v}_1) \cdot \mathbf{n})\mathbf{n}, \quad (2.47)$$

we have $\left| \frac{\partial(\mathbf{v}', \mathbf{v}'_1)}{\partial(\mathbf{v}, \mathbf{v}_1)} \right| = 1$ and equation (2.46) can be changed to

$$J = - \int_{R^3} \int_{R^3} \int_{S^2} \phi(\mathbf{v}') B(|\mathbf{v} - \mathbf{v}_1|, \theta) [f(\mathbf{v}') f(\mathbf{v}'_1) - f(\mathbf{v}) f(\mathbf{v}_1)] d\mathbf{n} d\mathbf{v}_1 d\mathbf{v}'. \quad (2.48)$$

From equations (2.45) and (2.48), we obtain

$$\begin{aligned} J &= \frac{1}{2} \int_{R^3} \int_{R^3} \int_{S^2} B(|\mathbf{v} - \mathbf{v}_1|, \theta) [\phi(\mathbf{v}) - \phi(\mathbf{v}')] \times \\ &\quad [f(\mathbf{v}') f(\mathbf{v}'_1) - f(\mathbf{v}) f(\mathbf{v}_1)] d\mathbf{n} d\mathbf{v}_1 d\mathbf{v}. \end{aligned} \quad (2.49)$$

Using the same argument, we obtain the following identity

$$\begin{aligned} &\int_{R^3} \int_{R^3} \int_{S^2} B(|\mathbf{v} - \mathbf{v}_1|, \theta) [\phi(\mathbf{v}) - \phi(\mathbf{v}')] f(\mathbf{v}) f(\mathbf{v}_1) d\mathbf{n} d\mathbf{v}_1 d\mathbf{v} \\ &= \int_{R^3} \int_{R^3} \int_{S^2} B(|\mathbf{v}' - \mathbf{v}'_1|, \theta) [\phi(\mathbf{v}') - \phi(\mathbf{v})] f(\mathbf{v}') f(\mathbf{v}'_1) d\mathbf{n} d\mathbf{v}'_1 d\mathbf{v}' \\ &= - \int_{R^3} \int_{R^3} \int_{S^2} B(|\mathbf{v} - \mathbf{v}_1|, \theta) [\phi(\mathbf{v}) - \phi(\mathbf{v}')] f(\mathbf{v}') f(\mathbf{v}'_1) d\mathbf{n} d\mathbf{v}_1 d\mathbf{v}. \end{aligned} \quad (2.50)$$

From equations (2.49) and (2.50), we have

$$J = \int_{R^3} \int_{R^3} \int_{S^2} B(|\mathbf{v} - \mathbf{v}_1|, \theta) [\phi(\mathbf{v}') - \phi(\mathbf{v})] f(\mathbf{v}) f(\mathbf{v}_1) d\mathbf{n} d\mathbf{v}_1 d\mathbf{v}. \quad (2.51)$$

By substitution $\phi(\mathbf{v}) = e^{-i2\pi\mathbf{k}\cdot\mathbf{v}}$ in equation (2.51), the Fourier transform on the velocity space of a collision integral $Q(f, f)$ can be written as

$$\begin{aligned} \int_{R^3} e^{-i2\pi\mathbf{k}\cdot\mathbf{v}} Q(f, f)(\mathbf{v}) d\mathbf{v} &= \int_{R^3} \int_{R^3} \int_{S^2} B(|\mathbf{v} - \mathbf{v}_1|, \theta) (e^{-i2\pi\mathbf{k}\cdot\mathbf{v}'} - e^{-i2\pi\mathbf{k}\cdot\mathbf{v}}) \times \\ &\quad f(\mathbf{v}) f(\mathbf{v}_1) d\mathbf{n} d\mathbf{v}_1 d\mathbf{v}. \end{aligned} \quad (2.52)$$

For ease of calculation, let us introduce new variables

$$\mathbf{u} = \mathbf{v} - \mathbf{v}_1, \quad \mathbf{s} = \frac{\mathbf{v} + \mathbf{v}_1}{2}.$$

Then

$$\mathbf{v}'_1 = \mathbf{s} - \frac{|\mathbf{u}\mathbf{n}|}{2}, \quad \mathbf{v}' = \mathbf{s} + \frac{|\mathbf{u}\mathbf{n}|}{2}.$$

We are interested in the case of Maxwell molecules with isotropic scattering where the scattering function B is of the form $B(|\mathbf{v} - \mathbf{v}_1|, \theta) = \frac{\sigma_0}{4\pi}$. By changing variables of integration

$$d\mathbf{v}_1 d\mathbf{v} = \left| \frac{\partial(\mathbf{v}_1, \mathbf{v})}{\partial(\mathbf{u}, \mathbf{s})} \right| d\mathbf{u} d\mathbf{s}$$

and $\left| \frac{\partial(\mathbf{v}_1, \mathbf{v})}{\partial(\mathbf{u}, \mathbf{s})} \right| = 1$, the integral on the right side of (2.52) can be written as

$$\begin{aligned} \frac{\sigma_0}{4\pi} \int_{R^3} \int_{R^3} f\left(\mathbf{s} + \frac{\mathbf{u}}{2}\right) f\left(\mathbf{s} - \frac{\mathbf{u}}{2}\right) |\mathbf{u}|^\gamma e^{-i2\pi\mathbf{k}\cdot\mathbf{s}} \\ \times \left[\int_{S^2} [e^{-i2\pi|\mathbf{u}|\mathbf{k}\cdot\mathbf{n}/2} - e^{-i2\pi\mathbf{k}\cdot\mathbf{u}/2}] d\mathbf{n} \right] d\mathbf{u} d\mathbf{s}. \end{aligned} \quad (2.53)$$

Using identity (see Appendix C)

$$\int_{S^2} [e^{-i2\pi|\mathbf{u}|\mathbf{k}\cdot\mathbf{n}/2} - e^{-i2\pi\mathbf{k}\cdot\mathbf{u}/2}] d\mathbf{n} = \int_{S^2} [e^{-i2\pi|\mathbf{k}|\mathbf{u}\cdot\mathbf{n}/2} - e^{-i2\pi\mathbf{k}\cdot\mathbf{u}/2}] d\mathbf{n},$$

the integral (2.53) becomes

$$\begin{aligned} \frac{\sigma_0}{4\pi} \int_{R^3} \int_{R^3} f\left(\mathbf{s} + \frac{\mathbf{u}}{2}\right) f\left(\mathbf{s} - \frac{\mathbf{u}}{2}\right) e^{-i2\pi\mathbf{k}\cdot\mathbf{s}} \\ \times \left[\int_{S^2} [e^{-i2\pi|\mathbf{k}|\mathbf{u}\cdot\mathbf{n}/2} - e^{-i2\pi\mathbf{k}\cdot\mathbf{u}/2}] d\mathbf{n} \right] d\mathbf{u} d\mathbf{s}. \end{aligned} \quad (2.54)$$

Let us introduce new variables

$$\mathbf{u} = \mathbf{x} - \mathbf{y}, \quad \mathbf{s} = \frac{1}{2}(\mathbf{x} + \mathbf{y})$$

then

$$d\mathbf{u}d\mathbf{s} = \left| \frac{\partial(\mathbf{u}, \mathbf{s})}{\partial(\mathbf{x}, \mathbf{y})} \right| d\mathbf{x}d\mathbf{y}$$

where the Jacobian is

$$\frac{\partial(\mathbf{u}, \mathbf{s})}{\partial(\mathbf{x}, \mathbf{y})} = \frac{\partial(u_1, u_2, u_3, s_1, s_2, s_3)}{\partial(x_1, x_2, x_3, y_1, y_2, y_3)} = \begin{vmatrix} \frac{1}{2} & 0 & 0 & \frac{1}{2} & 0 & 0 \\ 0 & \frac{1}{2} & 0 & 0 & \frac{1}{2} & 0 \\ 0 & 0 & \frac{1}{2} & 0 & 0 & \frac{1}{2} \\ -1 & 0 & 0 & 1 & 0 & 0 \\ 0 & -1 & 0 & 0 & 1 & 0 \\ 0 & 0 & -1 & 0 & 0 & 1 \end{vmatrix} = 1.$$

By using the new variables, the integral (2.54) becomes

$$\begin{aligned} & \frac{\sigma_0}{4\pi} \int_{R^3} \int_{R^3} f(\mathbf{x})f(\mathbf{y})e^{-i2\pi\mathbf{k}\cdot\frac{(\mathbf{x}+\mathbf{y})}{2}} \\ & \quad \times \left[\int_{S^2} [e^{-i2\pi\frac{(\mathbf{x}-\mathbf{y})}{2}\cdot|\mathbf{k}|\mathbf{n}} - e^{-i2\pi\frac{(\mathbf{x}-\mathbf{y})}{2}\cdot\mathbf{k}}]d\mathbf{n} \right] d\mathbf{y}d\mathbf{x} \\ &= \frac{\sigma_0}{4\pi} \int_{R^3} \int_{R^3} f(\mathbf{x})f(\mathbf{y}) \\ & \quad \times \left[\int_{S^2} [e^{-i2\pi\mathbf{x}\cdot\frac{(\mathbf{k}+|\mathbf{k}|\mathbf{n})}{2}} e^{-i2\pi\mathbf{y}\cdot\frac{(\mathbf{k}-|\mathbf{k}|\mathbf{n})}{2}} - e^{-i2\pi\mathbf{x}\cdot\mathbf{k}}]d\mathbf{n} \right] d\mathbf{y}d\mathbf{x} \\ &= \frac{\sigma_0}{4\pi} \int_{S^2} \left[\varphi\left(\frac{\mathbf{k}+|\mathbf{k}|\mathbf{n}}{2}\right) \varphi\left(\frac{\mathbf{k}-|\mathbf{k}|\mathbf{n}}{2}\right) - \varphi(\mathbf{k})\varphi(\mathbf{0}) \right] d\mathbf{n} \end{aligned} \quad (2.55)$$

Thus Fourier transform of the space homogeneous Boltzmann equation (2.43) for the case of Maxwell molecules with isotropic scattering can be written as

$$\begin{aligned} \frac{\partial\varphi}{\partial t}(\mathbf{x}, \mathbf{k}, t) &= \frac{\sigma_0}{4\pi} \int_{S^2} \left[\varphi\left(\mathbf{x}, \frac{\mathbf{k}+|\mathbf{k}|\mathbf{n}}{2}, t\right) \varphi\left(\mathbf{x}, \frac{\mathbf{k}-|\mathbf{k}|\mathbf{n}}{2}, t\right) \right. \\ & \quad \left. - \varphi(\mathbf{x}, \mathbf{k}, t)\varphi(\mathbf{x}, \mathbf{0}, t) \right] d\mathbf{n}, \end{aligned} \quad (2.56)$$

with the initial condition

$$\varphi(\mathbf{x}, \mathbf{k}, 0) = \int_{R^3} f(\mathbf{x}, \mathbf{v}, 0)e^{-i2\pi(\mathbf{v}\cdot\mathbf{k})}d\mathbf{v}. \quad (2.57)$$

2.5 Fourier Transform of the collision integral for Maxwell molecules. Case of a distribution function with cylindrical symmetry

Assume that the distribution function possess cylindrical symmetry with respect to velocity variable \mathbf{v} , that is

$$f(\mathbf{x}, \mathbf{v}, t) = f(\mathbf{x}, v_x, v_r, t)$$

where $\mathbf{v} = (v_x, v_y, v_z)$ and $v_r^2 = v_y^2 + v_z^2$. Then from Section (2.3), the Fourier transform with respect to the velocity variable \mathbf{v} of $f(\mathbf{x}, \mathbf{v}, t)$ denoted by $\varphi(\mathbf{x}, \mathbf{k}, t)$ also possess cylindrical symmetry and

$$\varphi(k_x, k_r) = 2\pi \int_{-\infty}^{\infty} e^{-i2\pi k_x v_x} \int_0^{\infty} J_0(2\pi k_r v_r) v_r f(v_x, v_r) dv_r dv_x \quad (2.58)$$

$$f(v_x, v_r) = 2\pi \int_{-\infty}^{\infty} e^{i2\pi k_x v_x} \int_0^{\infty} J_0(2\pi k_r v_r) v_r \varphi(k_x, k_r) dk_r dk_x. \quad (2.59)$$

We omit variables x and t which are not involved in the formula.

Let us consider the Fourier transform with respect to velocity variable of $Q(f, f)$ which is denoted by $\hat{Q}(\varphi, \varphi)$. From equation (2.56),

$$\hat{Q}(\varphi, \varphi) = \frac{\sigma_0}{4\pi} \int_{S^2} \left[\varphi\left(\frac{\mathbf{k} + |\mathbf{k}|\mathbf{n}}{2}\right) \varphi\left(\frac{\mathbf{k} - |\mathbf{k}|\mathbf{n}}{2}\right) - \varphi(\mathbf{k})\varphi(\mathbf{0}) \right] d\mathbf{n}. \quad (2.60)$$

Since $\varphi(\mathbf{k})$ possess cylindrical symmetry, we can write

$$\varphi\left(\frac{\mathbf{k} \pm |\mathbf{k}|\mathbf{n}}{2}\right) = \varphi\left(\frac{k_x \pm |\mathbf{k}|n_x}{2}, \left|\frac{\mathbf{k}_r \pm |\mathbf{k}|\mathbf{n}_r}{2}\right|\right) \quad (2.61)$$

where

$$\left|\frac{\mathbf{k}_r \pm |\mathbf{k}|\mathbf{n}_r}{2}\right| = \frac{1}{2} \sqrt{|\mathbf{k}_r|^2 + |\mathbf{k}|^2 |\mathbf{n}_r|^2 \pm 2|\mathbf{k}_r||\mathbf{n}_r||\mathbf{k}| \cos(\widehat{\mathbf{k}_r, \mathbf{n}_r})}$$

and

$$\begin{aligned} \mathbf{k} &= \mathbf{k}_x + \mathbf{k}_r, & \mathbf{k}_x &= k_x \mathbf{i}_x, & \mathbf{k}_r &= k_y \mathbf{i}_y + k_z \mathbf{i}_z \\ \mathbf{n} &= \mathbf{n}_x + \mathbf{n}_r, & \mathbf{n}_x &= n_x \mathbf{i}_x, & \mathbf{n}_r &= n_y \mathbf{i}_y + n_z \mathbf{i}_z. \end{aligned}$$

Let α be the azimuth angle measured counterclockwise for the vector \mathbf{k}_r to \mathbf{n}_r which is the projection of the vector \mathbf{n} , $\alpha \in [0, 2\pi)$ and β be the polar angle measured from the vector \mathbf{i}_x to \mathbf{n} , $\beta \in [0, \pi]$ as shown in Figure 2.2. Then

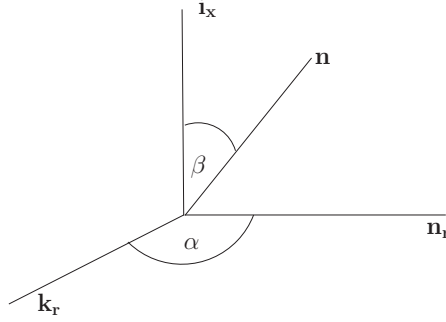


Figure 2.2 Angle between vectors.

$$n_x = \cos \beta, \quad |\mathbf{n}_r| = |\sin \beta|$$

and

$$\left| \frac{\mathbf{k}_r \pm |\mathbf{k}| \mathbf{n}_r}{2} \right| = \frac{1}{2} \sqrt{|\mathbf{k}_r|^2 + |\mathbf{k}|^2 \sin^2 \beta \pm 2|\mathbf{k}_r||\mathbf{k}| \sin \beta |\cos \alpha|}. \quad (2.62)$$

Let θ be angle between \mathbf{k} and \mathbf{n} then

$$\cos \theta = \frac{\mathbf{k} \cdot \mathbf{n}}{|\mathbf{k}|} = \frac{(k_x \cos \beta + |\mathbf{k}_r| |\sin \beta| \cos \alpha)}{|\mathbf{k}|}.$$

By substituting (2.62) and identity

$$\int_{S^2} d\mathbf{n} = \int_0^{2\pi} d\alpha \int_0^\pi d\beta \sin \beta. \quad (2.63)$$

to (2.60), we obtain

$$\begin{aligned} \hat{Q}(\varphi, \varphi) &= \frac{\sigma_0}{4\pi} \int_0^{2\pi} \int_0^\pi \sin \beta \\ &\times \left[\varphi \left(\frac{k_x + |\mathbf{k}| \cos \beta}{2}, \frac{1}{2} \sqrt{|\mathbf{k}_r|^2 + |\mathbf{k}|^2 \sin^2 \beta + 2|\mathbf{k}_r||\mathbf{k}| \sin \beta |\cos \alpha|} \right) \right. \\ &\times \varphi \left(\frac{k_x - |\mathbf{k}| \cos \beta}{2}, \frac{1}{2} \sqrt{|\mathbf{k}_r|^2 + |\mathbf{k}|^2 \sin^2 \beta - 2|\mathbf{k}_r||\mathbf{k}| \sin \beta |\cos \alpha|} \right) \\ &\left. - \varphi(k_x, |\mathbf{k}_r|) \varphi(\mathbf{0}) \right] d\beta d\alpha. \quad (2.64) \end{aligned}$$

For the sake of simplicity, let us write

$$\varphi_{\otimes, \odot}(\beta, \alpha) = \varphi \left(\frac{k_x \otimes |\mathbf{k}| \cos \beta}{2}, \frac{1}{2} \sqrt{|\mathbf{k}_r|^2 + |\mathbf{k}|^2 \sin^2 \beta \odot 2|\mathbf{k}_r||\mathbf{k}| \sin \beta \cos \alpha} \right) \quad (2.65)$$

where \otimes and \odot can be either $+$ or $-$. For example

$$\varphi_{+,-}(\beta, \alpha) = \varphi \left(\frac{k_x + |\mathbf{k}| \cos \beta}{2}, \frac{1}{2} \sqrt{|\mathbf{k}_r|^2 + |\mathbf{k}|^2 \sin^2 \beta - 2|\mathbf{k}_r||\mathbf{k}| \sin \beta \cos \alpha} \right).$$

From now on, we will omit parameters β and α for simplicity. Thus, equation (2.64) can be rewritten as

$$\hat{Q}(\varphi, \varphi) = \frac{\sigma_0}{4\pi} \int_0^{2\pi} \int_0^\pi \sin \beta [\varphi_{+,+}\varphi_{-,-} - \varphi(k_x, |\mathbf{k}_r|)\varphi(\mathbf{0})] d\beta d\alpha. \quad (2.66)$$

Let us write

$$\int_0^\pi \sin \beta \varphi_{+,+}\varphi_{-,-} d\beta = \int_0^{\frac{\pi}{2}} \sin \beta \varphi_{+,+}\varphi_{-,-} d\beta + \int_{\frac{\pi}{2}}^\pi \sin \beta \varphi_{+,+}\varphi_{-,-} d\beta. \quad (2.67)$$

By changing variable

$$\beta' = \beta - \pi$$

and using identities

$$\sin(\beta' + \pi) = -\sin \beta', \quad \cos(\beta' + \pi) = -\cos \beta'$$

then

$$\begin{aligned} \int_{\frac{\pi}{2}}^\pi \sin \beta \varphi_{+,+}\varphi_{-,-} d\beta &= - \int_{-\frac{\pi}{2}}^0 \sin \beta' \varphi_{-,+}\varphi_{+,-} d\beta' \\ &\stackrel{\beta' \rightarrow -\beta}{=} \int_0^{\frac{\pi}{2}} \sin \beta \varphi_{-,+}\varphi_{+,-} d\beta. \end{aligned} \quad (2.68)$$

The last integral is obtained by changing variable β' to $-\beta$.

Using equation (2.68), we have

$$\frac{\sigma_0}{4\pi} \int_0^{2\pi} \int_0^\pi \sin \beta \varphi_{+,+}\varphi_{-,-} d\beta d\alpha = \frac{\sigma_0}{4\pi} \int_0^{2\pi} \int_0^{\frac{\pi}{2}} \sin \beta [\varphi_{+,+}\varphi_{-,-} + \varphi_{+,-}\varphi_{-,+}] d\beta d\alpha. \quad (2.69)$$

Let us write

$$\begin{aligned} \int_0^{2\pi} [\varphi_{+,+}\varphi_{-,-} + \varphi_{+,-}\varphi_{-,+}] d\alpha &= \int_0^{\pi} [\varphi_{+,+}\varphi_{-,-} + \varphi_{+,-}\varphi_{-,+}] d\alpha \\ &+ \int_{\pi}^{2\pi} [\varphi_{+,+}\varphi_{-,-} + \varphi_{+,-}\varphi_{-,+}] d\alpha. \end{aligned} \quad (2.70)$$

By changing the variables

$$\alpha' = \alpha - \pi$$

and using identity

$$\cos(\alpha' + \pi) = -\cos \alpha',$$

we have

$$\begin{aligned} \varphi_{+,+} &\rightarrow \varphi_{+,-} \\ \varphi_{-,-} &\rightarrow \varphi_{-,+} \\ \varphi_{+,-} &\rightarrow \varphi_{+,+} \\ \varphi_{-,+} &\rightarrow \varphi_{-,-} \end{aligned} \quad (2.71)$$

and equation (2.70) becomes

$$\begin{aligned} \int_0^{2\pi} [\varphi_{+,+}\varphi_{-,-} + \varphi_{+,-}\varphi_{-,+}] d\alpha &= \int_0^{\pi} [\varphi_{+,+}\varphi_{-,-} + \varphi_{+,-}\varphi_{-,+}] d\alpha \\ &+ \int_0^{\pi} [\varphi_{+,-}\varphi_{-,+} + \varphi_{+,+}\varphi_{-,-}] d\alpha' \\ &= 2 \int_0^{\pi} [\varphi_{+,+}\varphi_{-,-} + \varphi_{+,-}\varphi_{-,+}] d\alpha \end{aligned} \quad (2.72)$$

where the notation “ \rightarrow ” means “change to”.

Consider

$$\begin{aligned} \int_0^{\pi} [\varphi_{+,+}\varphi_{-,-} + \varphi_{+,-}\varphi_{-,+}] d\alpha &= \int_0^{\frac{\pi}{2}} [\varphi_{+,+}\varphi_{-,-} + \varphi_{+,-}\varphi_{-,+}] d\alpha \\ &+ \int_{\frac{\pi}{2}}^{\pi} [\varphi_{+,+}\varphi_{-,-} + \varphi_{+,-}\varphi_{-,+}] d\alpha. \end{aligned} \quad (2.73)$$

Again by changing the variables

$$\alpha' = \alpha - \pi$$

and from (2.71), we obtain

$$\begin{aligned}
\int_0^\pi [\varphi_{+,+}\varphi_{-,-} + \varphi_{+,-}\varphi_{-,+}] d\alpha &= \int_0^{\frac{\pi}{2}} [\varphi_{+,+}\varphi_{-,-} + \varphi_{+,-}\varphi_{-,+}] d\alpha \\
&\quad + \int_{-\frac{\pi}{2}}^0 [\varphi_{+,-}\varphi_{-,+} + \varphi_{+,+}\varphi_{-,-}] d\alpha' \quad (2.74) \\
&= 2 \int_0^{\frac{\pi}{2}} [\varphi_{+,+}\varphi_{-,-} + \varphi_{+,-}\varphi_{-,+}] d\alpha.
\end{aligned}$$

The last integral is obtained by changing dummy variable α' to $-\alpha$. From equations (2.66, 2.69, 2.72, 2.74), we obtain

$$\hat{Q}(\varphi, \varphi) = \frac{\sigma_0}{\pi} \int_0^{\frac{\pi}{2}} \int_0^{\frac{\pi}{2}} \sin \beta [\varphi_{+,+}\varphi_{-,-} + \varphi_{+,-}\varphi_{-,+} - \varphi(k_x, |\mathbf{k}_r|)\varphi(\mathbf{0})] d\beta d\alpha. \quad (2.75)$$

Substitution of the expression for $\varphi_{+,+}, \varphi_{+,-}, \varphi_{-,+}$ and $\varphi_{-,-}$ yields

$$\begin{aligned}
\hat{Q}(\varphi, \varphi) &= \frac{\sigma_0}{4\pi} \int_0^{\frac{\pi}{2}} \int_0^\pi \sin \beta \\
&\quad \times \left[\varphi \left(\frac{k_x + |\mathbf{k}| \cos \beta}{2}, \frac{1}{2} \sqrt{|\mathbf{k}_r|^2 + |\mathbf{k}|^2 \sin^2 \beta + 2|\mathbf{k}_r||\mathbf{k}| \sin \beta \cos \alpha} \right) \right. \\
&\quad \times \varphi \left(\frac{k_x - |\mathbf{k}| \cos \beta}{2}, \frac{1}{2} \sqrt{|\mathbf{k}_r|^2 + |\mathbf{k}|^2 \sin^2 \beta - 2|\mathbf{k}_r||\mathbf{k}| \sin \beta \cos \alpha} \right) \\
&\quad + \varphi \left(\frac{k_x + |\mathbf{k}| \cos \beta}{2}, \frac{1}{2} \sqrt{|\mathbf{k}_r|^2 + |\mathbf{k}|^2 \sin^2 \beta - 2|\mathbf{k}_r||\mathbf{k}| \sin \beta \cos \alpha} \right) \\
&\quad \times \varphi \left(\frac{k_x - |\mathbf{k}| \cos \beta}{2}, \frac{1}{2} \sqrt{|\mathbf{k}_r|^2 + |\mathbf{k}|^2 \sin^2 \beta + 2|\mathbf{k}_r||\mathbf{k}| \sin \beta \cos \alpha} \right) \\
&\quad \left. - 2\varphi(k_x, |\mathbf{k}_r|)\varphi(\mathbf{0}) \right] d\beta d\alpha. \quad (2.76)
\end{aligned}$$

Introducing variable $\mu = \cos \beta$, then $|\sin \beta| = \sqrt{1 - \mu^2}$, we finally obtain

$$\begin{aligned}
\hat{Q}(\varphi, \varphi) = & \frac{\sigma_0}{\pi} \int_0^{\frac{\pi}{2}} \int_0^1 \\
& \left[\varphi \left(\frac{k_x + |\mathbf{k}|\mu}{2}, \frac{1}{2} \sqrt{|\mathbf{k}_r|^2 + |\mathbf{k}|^2(1 - \mu^2) + 2|\mathbf{k}_r||\mathbf{k}|\sqrt{1 - \mu^2} \cos \alpha} \right) \right. \\
& \times \varphi \left(\frac{k_x - |\mathbf{k}|\mu}{2}, \frac{1}{2} \sqrt{|\mathbf{k}_r|^2 + |\mathbf{k}|^2(1 - \mu^2) - 2|\mathbf{k}_r||\mathbf{k}|\sqrt{1 - \mu^2} \cos \alpha} \right) \\
& + \varphi \left(\frac{k_x + |\mathbf{k}|\mu}{2}, \frac{1}{2} \sqrt{|\mathbf{k}_r|^2 + |\mathbf{k}|^2(1 - \mu^2) - 2|\mathbf{k}_r||\mathbf{k}|\sqrt{1 - \mu^2} \cos \alpha} \right) \\
& \times \varphi \left(\frac{k_x - |\mathbf{k}|\mu}{2}, \frac{1}{2} \sqrt{|\mathbf{k}_r|^2 + |\mathbf{k}|^2(1 - \mu^2) + 2|\mathbf{k}_r||\mathbf{k}|\sqrt{1 - \mu^2} \cos \alpha} \right) \\
& \left. - 2\varphi(k_x, |\mathbf{k}_r|)\varphi(\mathbf{0}) \right] d\mu d\alpha. \quad (2.77)
\end{aligned}$$

CHAPTER III

NUMERICAL SCHEMES FOR PROBLEMS WITH RECTANGULAR SPACE GEOMETRY

3.1 General formulation of the problems

Consider the monatomic gas flow between two parallel flat plates which are separated by a distance L and have both infinite length and width as shown in the Figure (3.1). In the case of rarefied gas, the problem is stated for the Boltzmann

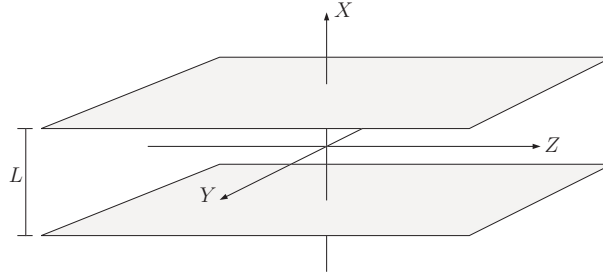


Figure 3.1 Flow between two flat plates.

equation (1.4). In this case, the distribution function $f(\mathbf{x}, \mathbf{v}, t)$ depends only on x, v_x, v_r and t where $\mathbf{x} = (x, y, z)$, $\mathbf{v} = (v_x, v_y, v_z)$ and $v_r^2 = v_y^2 + v_z^2$. For the Boltzmann equation one needs to state the initial conditions

$$f(\mathbf{x}, \mathbf{v}, 0) = f_0(\mathbf{x}, \mathbf{v}), \quad (3.1)$$

and the boundary conditions

$$\begin{cases} f(\frac{L}{2}, v_x, v_r) = n_+ \left(\frac{2\pi kT_2}{m}\right)^{-\frac{3}{2}} e^{-\frac{m}{2kT_2}(v_x^2 + v_r^2)}, & v_x < 0, \\ f(-\frac{L}{2}, v_x, v_r) = n_- \left(\frac{2\pi kT_1}{m}\right)^{-\frac{3}{2}} e^{-\frac{m}{2kT_1}(v_x^2 + v_r^2)}, & v_x > 0, \end{cases} \quad (3.2)$$

where

- T_1 and T_2 are the temperature at the bottom and top plates;
- n_+ and n_- are densities determined in calculations according to the total mass flow on the boundaries, $\int_{R^3} v_x f(x, \mathbf{v}) d\mathbf{v} = 0$, which corresponds to the impenetrable condition;
- k is the Boltzmann constant;
- m is the mass of a molecule.

3.2 Dimensionless analysis

All dimensionless variables are written with a “~”. The dimensional Boltzmann equation for the model of Maxwell molecules is

$$\frac{\partial f}{\partial t} + v_x \frac{\partial f}{\partial x} = \frac{\sigma_0}{4\pi} \int_{\mathbb{R}^3} \int_{S^2} [f(\mathbf{v}')f(\mathbf{v}'_1) - f(\mathbf{v})f(\mathbf{v}_1)] d\mathbf{n} d\mathbf{v}_1, \quad (3.3)$$

where the scattering function is $B = \frac{\sigma_0}{4\pi}$.

The dimensional and dimensionless variables are related by the formulae

$$f(t, x, v) = f_0 \tilde{f}(\tilde{t}, \tilde{x}, \tilde{v}), \quad t = t_0 \tilde{t}, \quad v = v_0 \tilde{v}, \quad x = x_0 \tilde{x}. \quad (3.4)$$

Using relations (3.4), the dimensional Boltzmann equation (3.3) is changed to dimensionless form

$$\frac{\partial \tilde{f}}{\partial \tilde{t}} + \tilde{v}_x \frac{\partial \tilde{f}}{\partial \tilde{x}} = \frac{1}{4\pi K n} \int_{\mathbb{R}^3} \int_{S^2} [f(\tilde{v}')f(\tilde{v}'_1) - f(\tilde{v})f(\tilde{v}_1)] d\mathbf{n} d\tilde{v}_1 \quad (3.5)$$

where $Kn = \frac{1}{\sigma_0 f_0 t_0 v_0^3}$.

The characteristic values are chosen as

$$f_0 = \bar{n} \left(\frac{kT_1}{m} \right)^{-\frac{3}{2}}, \quad t_0 = L \left(\frac{kT_1}{m} \right)^{-\frac{1}{2}}, \quad v_0 = \frac{L}{t_0} = \left(\frac{kT_1}{m} \right)^{\frac{1}{2}}, \quad x_0 = L, \quad (3.6)$$

where \bar{n} is mean density of the gas in the segment $[-\frac{L}{2}, \frac{L}{2}]$ and is equal to $\frac{1}{L} \int_{-\frac{L}{2}}^{\frac{L}{2}} n(x) dx$, $n(x)$ is the local gas density (1.18). The same scaling is applied to

the boundary conditions (3.2). The dimensionless form becomes

$$\begin{cases} \tilde{f}(\frac{1}{2}, \tilde{v}_x, \tilde{v}_r) = \tilde{n}_+ (2\pi T_+)^{-\frac{3}{2}} e^{-\frac{(\tilde{v}_x^2 + \tilde{v}_r^2)}{2T_+}}, & \tilde{v}_x < 0, \\ \tilde{f}(-\frac{1}{2}, \tilde{v}_x, \tilde{v}_r) = \tilde{n}_- (2\pi)^{-\frac{3}{2}} e^{-\frac{(\tilde{v}_x^2 + \tilde{v}_r^2)}{2}}, & \tilde{v}_x > 0, \end{cases} \quad (3.7)$$

where $T_+ = \frac{T_2}{T_1}$. For the sake of simplicity, we from now on omit the tilde symbol “~” from the top of the variables and understand that they are dimensionless.

3.3 Splitting algorithm

A new method is developed for solving the kinetic Boltzmann equation with cylindrical symmetry in the velocity space. The equations used are in dimensionless forms. By using the splitting method with respect to physical processes, the Boltzmann equation in each time layer is decomposed into the space homogeneous Boltzmann equation

$$\hat{f}_t = Q(\hat{f}, \hat{f}), \quad (3.8)$$

and the transport equation

$$f_t + v_x f_x = 0. \quad (3.9)$$

Equation (3.8) corresponds to a process of homogeneous relaxation through molecular collisions. Equation (3.9) describes free motion along molecular trajectories.

For the first equation (3.8) the initial conditions are

$$\hat{f}(x, v_x, v_r, t_n) = f(x, v_x, v_r, t_n). \quad (3.10)$$

For the second equation (3.9) the initial conditions are

$$f(x, v_x, v_r, t_n) = \hat{f}(x, v_x, v_r, t_n + \tau), \quad (3.11)$$

and the boundary conditions are given by equation (3.7).

For computing the distribution function $\hat{f}(\mathbf{x}, \mathbf{v}, t)$, the Fourier transform of the space homogeneous Boltzmann equation (2.56) is used,

$$\varphi_t = \hat{Q}(\varphi, \varphi). \quad (3.12)$$

In problems with rectangular space geometry, the distribution function has cylindrical symmetry in the velocity space

$$f = f(x, v_x, v_r, t).$$

3.4 Algorithm for heat transfer between parallel plates

By using the splitting method, we solve transport equation (3.9) and space homogeneous Boltzmann equation (3.8) simultaneously. We note here that the distribution function for this problem possess cylindrical symmetry in velocity space so that we can write

$$f = f(x, v_x, v_r, t)$$

where $v_r = \sqrt{v_y^2 + v_z^2}$. Using the fact from Section (2.3), the 3-dimensional Fourier transform of distribution function f denoted by φ also possess cylindrical symmetry in Fourier space so that we can write

$$\varphi = \varphi(x, k_x, k_r, t)$$

where $k_r = \sqrt{k_y^2 + k_z^2}$.

We remark that the n-dimensional Fourier transform can be calculated by applying the 1-dimensional Fourier transform to each dimension. Using this remark and the cylindrical symmetry of the velocity variables, the 3-dimensional Fourier transform on the velocity variable is equivalent to the 1-dimensional Fourier transform on the v_x variable and the Hankel transform on the v_r variable.

We consider two domains of computation. One is the physical domain in which we have to solve the transport equation. The other one is the Fourier domain in which we solve the relaxation problem. The two domains are related by Fourier transform as shown in Figure (3.2).

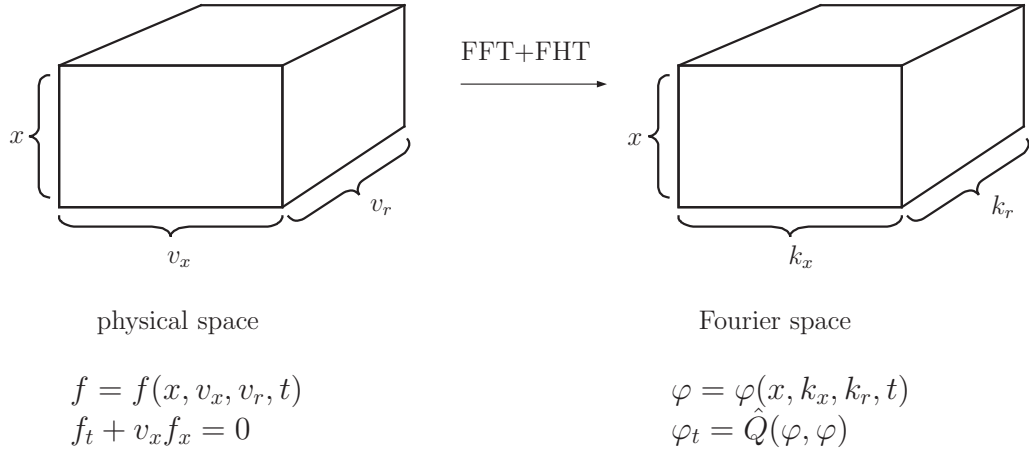


Figure 3.2 Realization of the splitting method.

3.4.1 Grid construction

Problems are considered for $x \in [-0.5, 0.5]$. We impose the assumption that the value of a distribution function in physical space is very small when $|v_x| > v_{x_{max}}$ or $v_r > v_{r_{max}}$. Thus we are interested in the case where $v_x \in [-v_{x_{max}}, v_{x_{max}})$ and $v_r \in [0, v_{r_{max}}]$. Let n_x, n_{v_x}, n_{v_r} be the number of grid points used in calculations along x, v_x and v_r directions, respectively. We note that n_{v_x} and n_{v_r} must be of the form of 2^n , for some $n \in \mathbb{N}$ in order to use the fast algorithm. Then the intervals $[-0.5, 0.5]$ for x and $[-v_{x_{max}}, v_{x_{max}})$ for v_x are divided equally into $n_x - 1$ and n_{v_x}

intervals so that

$$x_i = -0.5 + ih_x, \quad i = 0, 1, 2, \dots, n_x - 1,$$

$$v_{x,j} = -v_{x_{max}} + jh_{v_x}, \quad j = 0, 1, 2, \dots, n_{v_x} - 1,$$

where $h_x = \frac{1}{n_x - 1}$, $h_{v_x} = \frac{2v_{x_{max}}}{n_{v_x}}$.

The interval for k_x is related with $v_{x_{max}}$ and n_{v_x} . From Section (2.1.3), we have

$k_x \in [-k_{x_{max}}, k_{x_{max}}) = \left[-\frac{n_{v_x}}{4v_{x_{max}}}, \frac{n_{v_x}}{4v_{x_{max}}} \right)$ and this interval is discretized as

$$k_{x,j} = -\frac{n_{v_x}}{4v_{x_{max}}} + \frac{j}{2v_{x_{max}}}, \quad j = 0, 1, 2, \dots, n_{v_x} - 1.$$

In order to use the fast Hankel transform algorithm for the v_r direction, we need additional parameters:

- $v_{r_{min}}$ which determines the smallest value of v_r in physical space used in the fast Hankel transform algorithm.
- $k_{r_{min}}$ which determines the smallest value of k_r in Fourier space used in the fast Hankel transform algorithm.

Thus the computational domain for v_r is $[v_{r_{min}}, v_{r_{max}}]$. This interval is discretized exponentially as

$$v_{r,n_{v_r}-1-k} = v_{r_{max}} e^{-kh_r}, \quad k = 0, 1, 2, \dots, n_{v_r} - 1$$

where $h_r = \frac{1}{(n_{v_r} - 1)} \log \left(\frac{v_{r_{max}}}{v_{r_{min}}} \right)$.

The computational domain for k_r is $[k_{r_{min}}, k_{r_{max}}]$, where $k_{r_{max}} = k_{r_{min}} e^{(n_{v_r}-1)h_r}$, and it is discretized exponentially as

$$k_{r,k} = k_{r_{min}} e^{kh_r}, \quad k = 0, 1, 2, \dots, n_{v_r} - 1.$$

In this thesis, the parameters are chosen as follows,

$$r_{max} = k_{max} = 8$$

$$r_{min} = k_{min} = 0.001.$$

The space step h_x has to be chosen to satisfy the condition

$$h_x < Kn = \frac{\lambda}{L},$$

where λ is the mean free path of molecules.

3.4.2 Solving the transport problem in physical space

In physical space we solve transport equation

$$f_t + v_x f_x = 0, \quad (3.13)$$

with the initial conditions

$$f(x, v_x, v_r, 0) = f_0(x, v_x, v_r), \quad (3.14)$$

and the boundary conditions

$$\begin{cases} f(\frac{1}{2}, v_x, v_r) = n_+ (2\pi T_+)^{-\frac{3}{2}} e^{-\frac{(v_x^2 + v_r^2)}{2T_+}}, & v_x < 0, \\ f(-\frac{1}{2}, v_x, v_r) = n_- (2\pi)^{-\frac{3}{2}} e^{-\frac{(v_x^2 + v_r^2)}{2}}, & v_x > 0. \end{cases} \quad (3.15)$$

The parameters appearing in the boundary conditions are described in Section (3.1). For each v_x, v_r , we solve the transport equation using either the Lax-Wendroff or the upwind scheme depending on the following conditions.

case $v_x > 0$:

if $2 |f_{k,i,j}^\tau - f_{k-1,i,j}^\tau| > |f_{k+1,i,j}^\tau - 2f_{k,i,j}^\tau + f_{k-1,i,j}^\tau|$, then the Lax-Wendroff scheme is applied, otherwise the upwind scheme is used.

case $v_x < 0$:

if $2 |f_{k+1,i,j}^\tau - f_{k,i,j}^\tau| > |f_{k+1,i,j}^\tau - 2f_{k,i,j}^\tau + f_{k-1,i,j}^\tau|$, then the Lax-Wendroff scheme is applied, otherwise the upwind scheme is used.

The Lax-Wendroff scheme has the form

$$f_{k,i,j}^{\tau+1} = f_{k,i,j}^{\tau} - \frac{c}{2}(f_{k+1,i,j}^{\tau} - f_{k-1,i,j}^{\tau}) + \frac{c^2}{2}(f_{k+1,i,j}^{\tau} - 2f_{k,i,j}^{\tau} + f_{k-1,i,j}^{\tau}),$$

whereas in the upwind scheme

$$f_{k,i,j}^{\tau+1} = f_{k,i,j}^{\tau} - c(f_{k+1,i,j}^{\tau} - f_{k,i,j}^{\tau}),$$

where $c = \frac{\tau v_x}{h_x}$ is the Courant number.

We note that

1. the time step is τ ; k, i and j are indices along x, v_x and v_r , respectively;
2. for $v_x = 0$, the solution is the same as the initial conditions;
3. for calculating the boundary values, $f_{0,i,j}$ (corresponding to $x = -0.5$) and $f_{N_x-1,i,j}$ (corresponding to $x = 0.5$), we always use the upwind scheme;
4. On the boundaries, $x = 0.5$ and $x = -0.5$, the distribution function is calculated by numerical schemes only for molecules which are coming to the wall;
5. for stability of explicit schemes, we have to choose the time step τ such that the Courant number has to satisfy the condition $\frac{\tau |v_x|_{max}}{h_x} < 1$;
6. the Lax-Wendroff scheme is a second order of approximation $O(\tau^2, h_x^2)$, and the upwind scheme is a first order of approximation $O(\tau, h_x)$.

From remark 3, the solution on the boundaries is only defined in half of the velocity domain. The solution in the other half-spaces can be obtained by using the fact that mean velocity on the boundaries is zero (impenetrable condition),

$$\int_{-\infty}^{\infty} \int_0^{\infty} v_x v_r f(x, v_x, v_r, t) dv_r dv_x = 0. \quad (3.16)$$

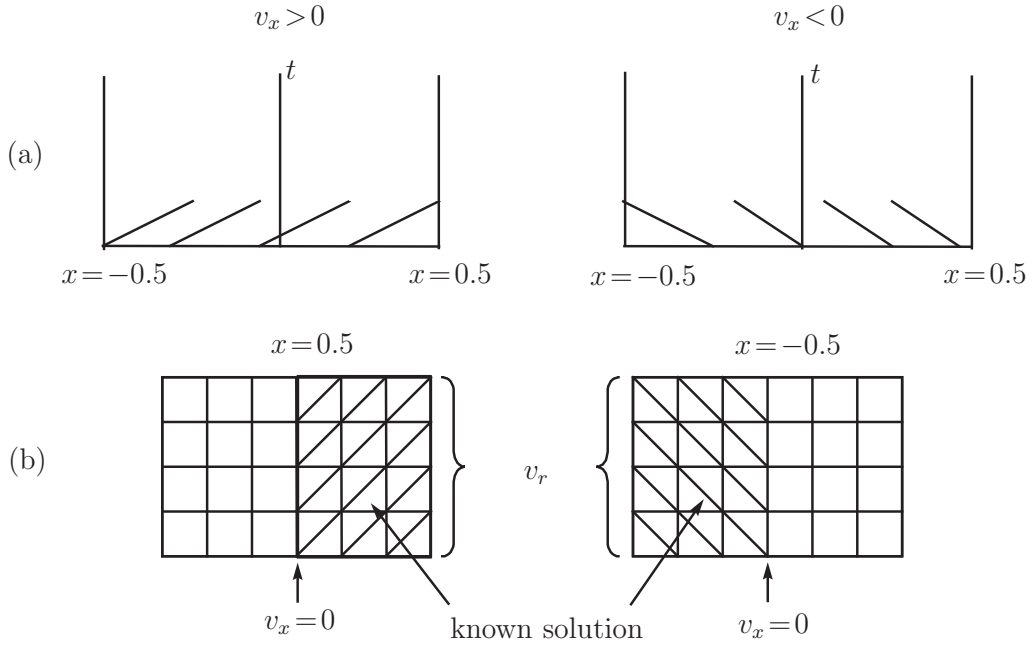


Figure 3.3 (a) Picture of characteristics. (b) Velocity domains where solution of (3.13) is found.

At $x = -0.5$;

$$n_- \int_0^\infty \int_0^\infty \frac{e^{-\frac{(v_x^2 + v_r^2)^2}{2}}}{(2\pi)^{3/2}} v_x v_r dv_r dv_x + \int_{-\infty}^0 \int_0^\infty f(-0.5, v_x, v_r) v_x v_r dv_r dv_x = 0. \quad (3.17)$$

At $x = 0.5$;

$$n_+ \int_{-\infty}^0 \int_0^\infty \frac{e^{-\frac{(v_x^2 + v_r^2)^2}{2T_+}}}{(2\pi T_+)^{3/2}} v_x v_r dv_r dv_x + \int_0^\infty \int_0^\infty f(0.5, v_x, v_r) v_x v_r dv_r dv_x = 0. \quad (3.18)$$

We note that f is the numerical solution obtained from solving transport equation (3.13). After calculating n_+ , n_- and taking into account the boundary conditions (3.15), we obtain a complete solution at the boundaries.

3.4.3 Solving the space homogeneous Boltzmann equation in the Fourier space

For each x , we solve the space homogeneous Boltzmann equation

$$\varphi_t = \hat{Q}(\varphi, \varphi) \quad (3.19)$$

with the initial conditions

$$\varphi(t_0, k_x, k_r) = \varphi_0(k_x, k_r). \quad (3.20)$$

For integration the problem (3.19), (3.20), we use the first order Runge-Kutta method. The first order Runge-Kutta method for equation (3.19), takes the form

$$\begin{aligned} k_1(k_x, k_r, t_n) &= \tau \hat{Q}(\varphi, \varphi) \\ &= \frac{\tau}{\pi K n} \int_0^{\frac{\pi}{2}} \int_0^1 [\varphi_{+,+} \varphi_{-,-} + \varphi_{+,-} \varphi_{-,+} - 2\varphi(k_x, k_r, t_n) \varphi(0, 0, t_n)] d\mu d\alpha, \end{aligned} \quad (3.21)$$

$$\varphi(k_x, k_r, t_{n+1}) = \varphi(k_x, k_r, t_n) + k_1(k_x, k_r, t_n),$$

where τ is the time step, $\varphi_{+,+}, \varphi_{+,-}, \varphi_{-,+}, \varphi_{-,-}$ are previously defined by (2.65). Note that not all points required for the calculation of $\varphi_{+,+}, \varphi_{+,-}, \varphi_{-,+}, \varphi_{-,-}$ (and also $\hat{\varphi}_{+,+}$, etc.) belong to our grid, so we need to do interpolation. In this thesis, spline interpolation is used. The integral is calculated numerically using two dimensional spline quadrature.

3.4.4 Relation of two stages of the splitting method

Let the distribution function $f(\mathbf{x}, \mathbf{v}, t_n)$ be given on the time layer $t = t_n$. This function $f(\mathbf{x}, \mathbf{v}, t_n)$ is used as the initial condition for the relaxation stage on the next time layer. This initial condition is transformed to the Fourier image space by using Fourier and Hankel transforms. We note that this transformation is independent of variable x , hence the algorithm can be easily implemented using

parallelization. The transformed function is used as the initial condition for the space homogeneous Boltzmann equation in the Fourier representation. After solving this equation, we transform the calculated result back to the physical space using inverse Fourier and Hankel transforms. The algorithm is depicted as in Figure (3.4). We note that the time step τ_v in the physical space is not necessary

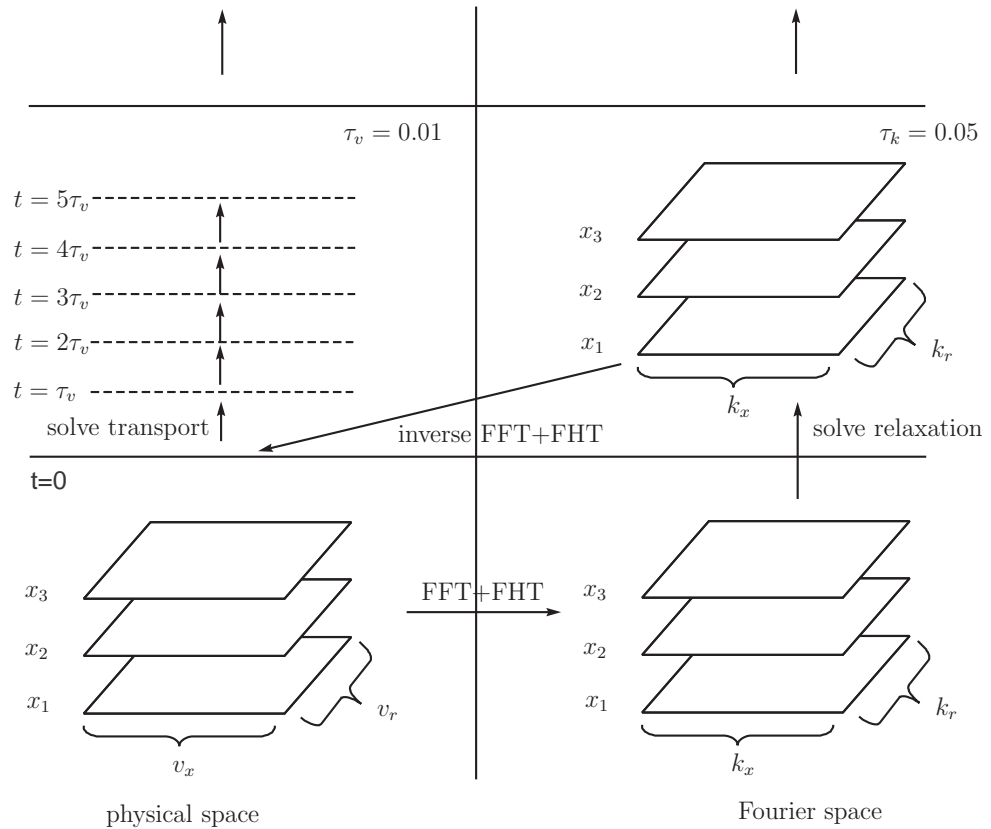


Figure 3.4 Connection between physical and Fourier space.

equal to τ_k in Fourier space. Since the computational time required for solving relaxation is much larger than that for solving the transport equation, we solve more than one step for the transport equation for each time step τ_k . For most calculations in the thesis, we use $\tau_k = 5\tau_v$ as shown in Figure (3.4).

3.5 Improvements of the algorithm

3.5.1 Conservation laws at the relaxation stage

For relaxation problems with cylindrical symmetry in the molecular velocity space we have conservation laws of mass (numerical density) $n(x, t)$, momentum along x -coordinate $n(x, t)U_x(x, t)$ and full energy $E(x, t)$ that are defined as follows

$$n(x, t) = 2\pi \int_{-\infty}^{\infty} \int_0^{\infty} v_r f(x, v_x, v_r, t) dv_r dv_x = C_1(x) \quad (3.22)$$

$$n(x, t)U_x(x, t) = 2\pi \int_{-\infty}^{\infty} \int_0^{\infty} v_x v_r f(x, v_x, v_r, t) dv_r dv_x = C_2(x) \quad (3.23)$$

$$\begin{aligned} E(x, t) &= 2\pi \int_{-\infty}^{\infty} \int_0^{\infty} v_r \left(\frac{v_x^2 + v_r^2}{2} \right) f(x, v_x, v_r, t) dv_r dv_x \\ &= \frac{3}{2}n(x, t)T(x, t) + \frac{1}{2}n(x, t)U_x^2(x, t) = C_3(x) \end{aligned} \quad (3.24)$$

where

$$\frac{3}{2}n(x, t)T(x, t) = 2\pi \int_{-\infty}^{\infty} \int_0^{\infty} v_r \left(\frac{c_x^2 + v_r^2}{2} \right) f(x, v_x, v_r, t) dv_r dv_x, \quad (3.25)$$

and

$$c_x = v_x - U_x(x, t)$$

is a heat velocity along the x -coordinate.

In the Fourier representation

$$\varphi(x, k_x, k_r, t) = 2\pi \int_{-\infty}^{\infty} e^{-i2\pi k_x v_x} \int_0^{\infty} v_r J_0(2\pi k_r v_r) f(x, v_x, v_r, t) dv_r dv_x, \quad (3.26)$$

the mass conservation law has the form

$$\varphi(x, 0, 0, t) = n(x, t) = 2\pi \int_{-\infty}^{\infty} \int_0^{\infty} v_r f(x, v_x, v_r, t) dv_r dv_x = C_1(x). \quad (3.27)$$

Taking cylindrical symmetry into account, the differential gradient operator and the Laplace operator take the form

$$\nabla_{\mathbf{k}} = \mathbf{e}_x \partial_{k_x} + \mathbf{e}_r \partial_{k_r}, \quad \Delta_{\mathbf{k}} = \partial_{k_x}^2 + \frac{1}{k_r} \partial_{k_1} (k_1 \partial_{k_1}).$$

Differentiating equation (3.26), and using identities

$$\frac{d}{dx}J_0(x) = -J_1(x), \quad \frac{d}{dx}[xJ_1(x)] = xJ_0(x), \quad (3.28)$$

we obtain the next expression for the conservation law

$$\begin{aligned} \nabla\varphi|_{|\mathbf{k}|=0} &= -4\pi^2 i\mathbf{e}_x \int_{-\infty}^{\infty} \int_0^{\infty} v_x v_r f(x, v_x, v_r, t) dv_r dv_x \\ &= -2\pi i\mathbf{e}_x n(x, t) U_x(x, t) = C_4(x)\mathbf{e}_x, \end{aligned} \quad (3.29)$$

$$\begin{aligned} \frac{1}{2}\Delta\varphi|_{|\mathbf{k}|=0} &= -4\pi^2 \left(2\pi \int_{-\infty}^{\infty} \int_0^{\infty} v_r \left(\frac{v_x^2 + v_r^2}{2} \right) f(x, v_x, v_r, t) dv_r dv_x \right) \\ &= -4\pi^2 \left(\frac{3}{2}nT + \frac{1}{2}nU_x^2 \right) = C_5(x). \end{aligned} \quad (3.30)$$

From now on, some independent variables will be omitted. To derive equations (3.29) and (3.30), consider

$$\frac{\partial\varphi}{\partial k_r}(k_x, k_r) = -4\pi^2 \int_{-\infty}^{\infty} \int_0^{\infty} e^{-i2\pi v_x k_x} v_r^2 J_1(2\pi k_r v_r) f(v_x, v_r) dv_r dv_x, \quad (3.31)$$

$$\frac{\partial^2\varphi}{\partial k_r^2}(k_x, k_r) = -4\pi^2 \int_{-\infty}^{\infty} \int_0^{\infty} e^{-i2\pi v_x k_x} v_r^2 \left(\frac{\partial}{\partial k_r} J_1(2\pi k_r v_r) \right) f(v_x, v_r) dv_r dv_x. \quad (3.32)$$

Since

$$\begin{aligned} \frac{d}{dk_r}[J_1(2\pi k_r v_r)] &= \frac{d}{dk_r} \left[\frac{k_r J_1(2\pi k_r v_r)}{k_r} \right] \\ &= k_r J_1(2\pi k_r v_r) \left(-\frac{1}{k_r^2} \right) + \frac{1}{k_r} \frac{d}{dk_r} [k_r J_1(2\pi k_r v_r)] \\ &= -\frac{J_1(2\pi k_r v_r)}{k_r} + 2\pi v_r J_0(2\pi k_r v_r) \end{aligned} \quad (3.33)$$

therefore equation (3.32) becomes

$$\begin{aligned} \frac{\partial^2\varphi}{\partial k_r^2}(k_x, k_r) &= 4\pi^2 \int_{-\infty}^{\infty} \int_0^{\infty} e^{-i2\pi v_x k_x} v_r^2 \left(\frac{J_1(2\pi k_r v_r)}{k_r} - 2\pi v_r J_0(2\pi k_r v_r) \right) \\ &\quad \times f(v_x, v_r) dv_r dv_x. \end{aligned} \quad (3.34)$$

Differentiating equation (3.26) with respect to k_x yields

$$\frac{\partial}{\partial k_x} \varphi(k_x, k_r) = -4\pi^2 i \mathbf{e}_x \int_{-\infty}^{\infty} \int_0^{\infty} e^{-i2\pi k_x v_x} v_x v_r J_0(2\pi k_r v_r) f(x, v_x, v_r, t) dv_r dv_x, \quad (3.35)$$

$$\frac{\partial^2}{\partial k_x^2} \varphi(k_x, k_r) = -8\pi^3 \int_{-\infty}^{\infty} \int_0^{\infty} e^{-i2\pi k_x v_x} v_x^2 v_r J_0(2\pi k_r v_r) f(v_x, v_r) dv_r dv_x. \quad (3.36)$$

Using equations (3.31) and (3.35), the conservation law equation (3.29) can be obtained. From equations (3.31), (3.34) and (3.36) we obtain

$$\Delta \varphi = -8\pi^3 \int_{-\infty}^{\infty} \int_0^{\infty} e^{-i2\pi k_x v_x} (v_x^2 + v_r^2) v_r J_0(2\pi k_r v_r) f(v_x, v_r) dv_r dv_x. \quad (3.37)$$

The conservation law equation (3.30) can be obtained by using equation (3.37).

3.5.2 Discrete conservation laws

The Fourier- representation of the Boltzmann equation at the relaxation stage is

$$\frac{\partial \varphi}{\partial t} = \frac{1}{4\pi K n} \int_0^{2\pi} \int_0^{\pi} \sin \beta [\varphi_+(k_x, k_r) \varphi_-(k_x, k_r) - \varphi(k_x, k_r) \varphi(0, 0)] d\beta d\alpha, \quad (3.38)$$

where

$$\varphi_{\pm}(k_x, k_r) = \varphi \left(\frac{1}{2}(k_x \pm |\mathbf{k}| \cos \beta), \frac{1}{2} \sqrt{(k_r^2 \pm 2k_r |\mathbf{k}| \sin \beta \cos \alpha + |\mathbf{k}|^2 \sin^2 \beta)} \right). \quad (3.39)$$

One can show that the Runge-Kutta scheme of any order for (3.38) with the initial condition

$$\varphi(\mathbf{k}, 0) = \varphi_0(\mathbf{k}), \quad (3.40)$$

conserves the density, that is

$$\varphi(\mathbf{0}, \tau) = \varphi_0(\mathbf{0}), \quad (3.41)$$

where τ is the time step.

3.5.3 Asymptotic solution of the relaxation problem near zero grid point

The Taylor series expansion of the function $\varphi(h_x, h_r)$ for small h_x, h_r is

$$\varphi(h_x, h_r, t) = \varphi(t, 0, 0) + \delta\varphi|_{|\mathbf{k}|=0} + \frac{1}{2}\delta^2\varphi|_{|\mathbf{k}|=0} + O(|\mathbf{k}|^3), \quad (3.42)$$

where h_x, h_r are spacings along corresponding coordinates of grid points nearest to zero, δ, δ^2 are differentials of first and second order. Taking cylindrical symmetry and equation (3.29) into account,

$$\delta\varphi|_{|\mathbf{k}|=0} = -2\pi inU_x h_x, \quad (3.43)$$

$$\delta^2\varphi|_{|\mathbf{k}|=0} = \partial_{k_x}^2\varphi|_{|\mathbf{k}|=0}h_x^2 + \partial_{k_r}^2\varphi|_{|\mathbf{k}|=0}h_r^2. \quad (3.44)$$

We have

$$\partial_{k_x}^2\varphi|_{|\mathbf{k}|=0}h_x^2 = -4\pi^2 n (U_x h_x)^2 - 4\pi^2 \left[2\pi \int_{-\infty}^{\infty} \int_0^{\infty} v_r c_x^2 f(v_x, v_r) dv_r dv_x \right] h_x^2, \quad (3.45)$$

$$\partial_{k_r}^2\varphi|_{|\mathbf{k}|=0}h_r^2 = -4\pi^2 \left[2\pi \int_{-\infty}^{\infty} \int_0^{\infty} \frac{1}{2} v_r^3 f(v_x, v_r) dv_r dv_x \right] h_r^2. \quad (3.46)$$

Equation (3.46) is obtained by using (3.28) and the identity

$$J_1(x) = \frac{1}{2}x(J_0(x) + J_2(x)). \quad (3.47)$$

Let us introduce notations

$$nT_x = 2\pi \int_{-\infty}^{\infty} \int_0^{\infty} v_r \frac{1}{2} c_x^2 f(x, t, v_x, v_r) dv_r dv_x, \quad (3.48)$$

$$nT_r = 2\pi \int_{-\infty}^{\infty} \int_0^{\infty} \frac{1}{2} v_r^3 f(x, t, v_x, v_r) dv_r dv_x. \quad (3.49)$$

Then from equation (3.25) we have

$$\frac{3}{2}T(x, t) = T_x(x, t) + T_r(x, t). \quad (3.50)$$

Using equations (3.42), (3.45), (3.46) and (3.50) one obtains

$$\begin{aligned}\varphi(h_x, h_r) &= n - 2\pi in U_x h_x - 2\pi^2 n \left((U_x h_x)^2 + 2T_x h_x^2 + T_r h_r^2 \right) + O(h^3) \\ &= n - 2\pi in U_x h_x - 2\pi^2 n \left((U_x h_x)^2 + \frac{3}{2} h_r^2 T + T_x (2h_x^2 - h_r^2) \right) + O(h^3).\end{aligned}\tag{3.51}$$

Differentiating equation (3.51) with respect to t and taking into account the conservation laws (3.27), (3.29), (3.30), we obtain

$$\frac{\partial \varphi}{\partial t} = -2\pi^2 n (2h_x^2 - h_r^2) \dot{T}_x + O(h^3),\tag{3.52}$$

where we denote by the dot symbol the time derivative of function T_x . Using equations (3.51) and (3.39), the brackets in the integrand of the collision integral in equation (3.38) can be calculated with accuracy up to $O(h^3)$ as

$$\begin{aligned}[\varphi_+(h_x, h_r)\varphi_-(h_x, h_r) - \varphi(h_x, h_r)\varphi(0, 0)] &= \frac{3}{4} n^2 \pi^2 (T - 2T_x) [h_r^2 - h_x^2 + \\ &\quad (h_r^2 + h_x^2) \cos(2\beta)] + O(h^3).\end{aligned}\tag{3.53}$$

Substituting equation (3.53) into (3.38), we obtain

$$\frac{\partial \varphi}{\partial t} = \frac{n^2 \pi^2}{2Kn} (h_r^2 - 2h_x^2) (T - 2T_x).\tag{3.54}$$

Equating equations (3.52) and (3.54), we get

$$2\dot{T}_x + \frac{n}{Kn} T_x = \frac{n}{2Kn} T.\tag{3.55}$$

The solution of (3.55) is given by

$$T_x(t) = \frac{T}{2} + \left(T_x(0) - \frac{T}{2} \right) e^{-\frac{nt}{2Kn}}.\tag{3.56}$$

3.5.4 Numerical procedure

Let us consider the computation on the next $(p+1)$ -time step starts from relaxation stage. At the end of the computations on the previous p -time step, the

integrals (3.22)-(3.24) and (3.48) are calculated. As a result we have sets of values

$$n_m^p, \quad n_m^p U_{x,m}^p, \quad T_m^p, \quad T_{x,m}^p.$$

These values will be used to improve the value of the distribution function on the grid points

$$(0, 0), \quad (\pm h_x, 0), \quad (0, h_1), \quad (\pm h_x, h_1).$$

Using (3.51), we have

$$\varphi_m^{p+1}(0, 0) = n_m^p, \quad (3.57)$$

$$\varphi_m^{p+1}(\pm h_x, 0) = n_m^p - 2\pi i n_m^p U_{x,m}^p(\pm h_x) - 2\pi^2 n_m^p \left[(U_{x,m}^p h_x)^2 + 2T_{x,m}^{p+1} h_x^2 \right], \quad (3.58)$$

$$\varphi_m^{p+1}(0, h_r) = n_m^p - 2\pi^2 n_m^p T_{r,m}^{p+1} h_r^2, \quad (3.59)$$

$$\begin{aligned} \varphi_m^{p+1}(\pm h_x, h_r) = n_m^p - 2\pi i n_m^p U_{x,m}^p(\pm h_x) - 2\pi^2 n_m^p \left[(U_{x,m}^p h_x)^2 + \frac{3}{2} h_r^2 T_m^p \right. \\ \left. + (2h_x^2 - h_r^2) T_{x,m}^{p+1} \right]. \end{aligned} \quad (3.60)$$

Here according to (3.56),

$$T_{x,m}^{p+1} = \frac{T_m^p}{2} + \left(T_{x,m}^p - \frac{T_m^p}{2} \right) e^{-\frac{n_m^p \tau}{2Kn}} \quad (3.61)$$

where τ is the time step. Using (3.50), we obtain

$$T_{r,m}^{p+1} = \frac{3}{2} T_m^p - T_{x,m}^{p+1}. \quad (3.62)$$

For small τ , instead of (3.61) we can use an asymptotic expansion

$$T_{x,m}^{p+1} = \frac{T_m^p n_m^p \tau}{4Kn} + T_{x,m}^p \left(1 - \frac{n_m^p \tau}{2Kn} \right). \quad (3.63)$$

For the heat transfer problem between parallel plates, we have $U_x = 0$. To fulfill such a conservation law up to $O(h_x^2)$ we need to align

$$\varphi_m^{p+1}(h_x, 0) = \varphi_m^{p+1}(-h_x, 0). \quad (3.64)$$

CHAPTER IV

RESULTS, DISCUSSION AND CONCLUSION

4.1 Qualitative behavior of the solution of problems with rectangular geometry

In the case of Maxwell molecules, there are no regular data for comparison of the heat transfer problem. Hence, it is useful to obtain estimates of behavior of profiles of hydrodynamic variables.

4.1.1 Comparative behavior of hydrodynamic profiles for different types of molecules

Let us transform the Boltzmann equation for Maxwellian molecules and hard sphere model

$$\begin{aligned} \left(\frac{dn}{dx}\right)_i &= \frac{d}{dx} \left(\int_{R^3} f(x, \mathbf{v}) d\mathbf{v} \right), \\ &= \int_{R^3} \frac{1}{v_x} c_i Q_i(f, f) d\mathbf{v}, \end{aligned} \quad (4.1)$$

where $i = 1$ corresponds to Maxwellian molecules and $i = 2$ for hard sphere molecules. Here

$$Q_1 = \int_{R^3} \int_{S^2} [f' f'_1 - f f_1] d\mathbf{n} d\mathbf{v}_1, \quad (4.2)$$

$$Q_2 = \int_{R^3} \int_{S^2} |\mathbf{v} - \mathbf{v}_1| [f' f'_1 - f f_1] d\mathbf{n} d\mathbf{v}_1, \quad (4.3)$$

and $c_1 = \frac{1}{4\pi Kn}$, $c_2 = \frac{1}{\sqrt{2}\pi Kn_s}$. In our calculations we accept $c_1 = c_2$. Using the Cauchy-Schwarz inequality, we estimate for hard sphere molecules

$$\begin{aligned} & \left| \int_{R^3} \int_{R^3} \int_{S^2} \frac{1}{v_x} |\mathbf{v} - \mathbf{v}_1| [f' f'_1 - f f_1] \frac{\sqrt{f_0(\mathbf{v}) f_0(\mathbf{v}_1)}}{\sqrt{f_0(\mathbf{v}) f_0(\mathbf{v}_1)}} d\mathbf{n} d\mathbf{v}_1 d\mathbf{v} \right| \\ & \leq \left[\int_{R^3} \int_{R^3} \int_{S^2} \left(|\mathbf{v} - \mathbf{v}_1| \sqrt{f_0(\mathbf{v}) f_0(\mathbf{v}_1)} \right)^2 d\mathbf{n} d\mathbf{v}_1 d\mathbf{v} \right]^{\frac{1}{2}} \\ & \times \left[\int_{R^3} \int_{R^3} \int_{S^2} \frac{1}{v_x^2} [f' f'_1 - f f_1]^2 \left(\frac{1}{\sqrt{f_0(\mathbf{v}) f_0(\mathbf{v}_1)}} \right)^2 d\mathbf{n} d\mathbf{v}_1 d\mathbf{v} \right]^{\frac{1}{2}}. \end{aligned} \quad (4.4)$$

For Maxwellian molecules,

$$\begin{aligned} & \left| \int_{R^3} \int_{R^3} \int_{S^2} \frac{1}{v_x} [f' f'_1 - f f_1] \frac{\sqrt{f_0(\mathbf{v}) f_0(\mathbf{v}_1)}}{\sqrt{f_0(\mathbf{v}) f_0(\mathbf{v}_1)}} d\mathbf{n} d\mathbf{v}_1 d\mathbf{v} \right| \\ & \leq \left[\int_{R^3} \int_{R^3} \int_{S^2} \left(\sqrt{f_0(\mathbf{v}) f_0(\mathbf{v}_1)} \right)^2 d\mathbf{n} d\mathbf{v}_1 d\mathbf{v} \right]^{\frac{1}{2}} \\ & \times \left[\int_{R^3} \int_{R^3} \int_{S^2} \frac{1}{v_x^2} [f' f'_1 - f f_1]^2 \left(\frac{1}{\sqrt{f_0(\mathbf{v}) f_0(\mathbf{v}_1)}} \right)^2 d\mathbf{n} d\mathbf{v}_1 d\mathbf{v} \right]^{\frac{1}{2}}. \end{aligned} \quad (4.5)$$

From these estimates we obtain

$$\begin{aligned} \left| \left(\frac{dn}{dx} \right)_2 \right| & \leq c_2 \left[\int_{R^3} \int_{R^3} \int_{S^2} f_0(\mathbf{v}) f_0(\mathbf{v}_1) |\mathbf{v} - \mathbf{v}_1|^2 d\mathbf{n} d\mathbf{v}_1 d\mathbf{v} \right]^{\frac{1}{2}} \times F_2, \\ \left| \left(\frac{dn}{dx} \right)_1 \right| & \leq c_1 \left[\int_{R^3} \int_{R^3} \int_{S^2} f_0(\mathbf{v}) f_0(\mathbf{v}_1) d\mathbf{n} d\mathbf{v}_1 d\mathbf{v} \right]^{\frac{1}{2}} \times F_2, \end{aligned} \quad (4.6)$$

where

$$F_2 = \left[\int_{R^3} \int_{R^3} \int_{S^2} \frac{1}{v_x^2} [f' f'_1 - f f_1]^2 \frac{1}{f_0(\mathbf{v}) f_0(\mathbf{v}_1)} d\mathbf{n} d\mathbf{v}_1 d\mathbf{v} \right]^{\frac{1}{2}}. \quad (4.7)$$

Note that

$$\int_{R^3} \int_{R^3} \int_{S^2} f_0(\mathbf{v}) f_0(\mathbf{v}_1) |\mathbf{v} - \mathbf{v}_1|^2 d\mathbf{n} d\mathbf{v}_1 d\mathbf{v} = 4\pi n^2 F_1, \quad (4.8)$$

$$\int_{R^3} \int_{R^3} \int_{S^2} f_0(\mathbf{v}) f_0(\mathbf{v}_1) d\mathbf{n} d\mathbf{v}_1 d\mathbf{v} = 4\pi n^2, \quad (4.9)$$

where

$$F_1 = \frac{1}{(2\pi)^3} \int_{R^3} \int_{R^3} e^{-\frac{v^2 + v_1^2}{2}} |\mathbf{v} - \mathbf{v}_1|^2 d\mathbf{v}_1 d\mathbf{v}. \quad (4.10)$$

The last integral is calculated in Appendix B:

$$F_1 = 6.$$

Hence,

$$\left| \frac{1}{n} \left(\frac{dn}{dx} \right)_1 \right| \leq 2\sqrt{\pi}F_2, \quad (4.11)$$

$$\left| \frac{1}{n} \left(\frac{dn}{dx} \right)_2 \right| \leq \sqrt{6}(2\sqrt{\pi}F_2). \quad (4.12)$$

These estimates indirectly explain the comparative behavior of the calculated results and the results known from literature for hard sphere molecules. One can obtain similar estimates for temperature profiles.

Similar estimates are valid for other problems with rectangular geometry. For example, the recondensation problem between parallel plates, shock wave structure and others.

Let us also give some other approximate estimates. Using the generalized mean value theorem, we rewrite (4.1) as

$$\left(\frac{dn}{dx} \right)_1 = S_1 \times I_1, \quad (4.13)$$

$$\left(\frac{dn}{dx} \right)_2 = S_2 \times I_2, \quad (4.14)$$

where

$$S_1 = \left[\frac{1}{v_x} \frac{[f'f'_1 - ff_1]}{f_0(\mathbf{v})f_0(\mathbf{v}_1)} \right]_{\mathbf{v}=\mathbf{v}_*, \mathbf{v}_1=\mathbf{v}_{1*}}, \quad (4.15)$$

$$S_2 = \left[\frac{1}{v_x} \frac{[f'f'_1 - ff_1]}{f_0(\mathbf{v})f_0(\mathbf{v}_1)} \right]_{\mathbf{v}=\tilde{\mathbf{v}}_*, \tilde{\mathbf{v}}_1=\tilde{\mathbf{v}}_{1*}}, \quad (4.16)$$

$$I_1 = \int_{R^3} \int_{R^3} \int_{S^2} f_0(\mathbf{v})f_0(\mathbf{v}_1)d\mathbf{n}d\mathbf{v}_1d\mathbf{v}, \quad (4.17)$$

$$I_2 = \int_{R^3} \int_{R^3} \int_{S^2} f_0(\mathbf{v})f_0(\mathbf{v}_1)|\mathbf{v} - \mathbf{v}_1|d\mathbf{n}d\mathbf{v}_1d\mathbf{v}. \quad (4.18)$$

Since the Boltzmann brackets are normalized by the production of Maxwellian functions, one can assume that

$$|S_1| \approx |S_2|.$$

Then

$$\left| \left(\frac{dn}{dx} \right)_2 \right| \approx \frac{4}{\sqrt{\pi}} \left| \left(\frac{dn}{dx} \right)_1 \right|. \quad (4.19)$$

Similar estimates are valid for temperature profiles. The same behavior of profiles of hydrodynamics variables was observed in comparisons of our results with the results for hard sphere molecules.

4.2 Testing the splitting method stages

Each part of the algorithm was tested separately before applying it to the classical problems of rarefied gas dynamics. All computations were performed with double-precision arithmetic on Unix operating system. To compare numerical results with exact values, the relative L_∞ -norm of error in a discrete function space which is defined as

$$\|f^{(numerical)} - f^{(exact)}\|_{L_\infty} = \frac{\max |f^{(numerical)} - f^{(exact)}|}{\max |f^{(exact)}|},$$

is used.

4.2.1 Testing finite-difference schemes for the transport stage

In this section we consider the typical initial-boundary value problem. This problem is a good test for choosing a corresponding scheme. The problem consists of the transport equation (3.13)

$$f_t + v_x f_x = 0, \quad (4.20)$$

the boundary conditions (3.7)

$$\begin{cases} f(\frac{1}{2}, v_x, v_r, t) = \frac{2\nu}{1+\nu} (2\pi T_+)^{-\frac{3}{2}} e^{-\frac{(v_x^2+v_r^2)}{2T_+}}, & v_x < 0, \\ f(-\frac{1}{2}, v_x, v_r, t) = \frac{2}{1+\nu} (2\pi)^{-\frac{3}{2}} e^{-\frac{(v_x^2+v_r^2)}{2}}, & v_x > 0, \end{cases} \quad (4.21)$$

and the initial conditions

$$f_0(x, v_x, v_r) = \begin{cases} f(\frac{1}{2}, v_x, v_r), & v_x < 0, \\ f(-\frac{1}{2}, v_x, v_r), & v_x > 0, \\ \frac{1}{2} [f(\frac{1}{2}, v_x, v_r) + f(-\frac{1}{2}, v_x, v_r)], & v_x = 0, \end{cases} \quad (4.22)$$

where $\nu = \frac{n_+}{n_-}$.

The function $f(x, v_x, v_r, t) = f_0(x, v_x, v_r)$ is an exact stationary solution of the Boltzmann equation (1.4), which gives zero value for the collision integral. Therefore it is called the free molecular solution (Kogan, 1969). This solution has the following hydrodynamics variables:

1. Molecular flow in each grid point x_n is equal to zero (Kogan, 1969), i.e.,

$$nU_x = \int_{R^3} v_x f_0(x_n, \mathbf{v}) d\mathbf{v} = 0.$$

From this condition, one obtains

$$\nu = \frac{1}{\sqrt{T_+}}.$$

This also means that the mean velocity is zero.

2. Density, temperature and heat flux are constant. They are

$$n(x_n) = \int_{R^3} f(x_n, \mathbf{v}) d\mathbf{v} = \frac{1}{2}(n_+ + n_-) = 1, \quad (4.23)$$

$$T(x_n) = \frac{2}{3n(x_n)} \int_{R^3} \mathbf{v}^2 f(x_n, \mathbf{v}) d\mathbf{v} = 2\sqrt{T_+}, \quad (4.24)$$

$$q_x(x_n) = \frac{1}{2} \int_{R^3} v_x \mathbf{v}^2 f(x_n, \mathbf{v}) d\mathbf{v} = -2\sqrt{\frac{2}{\pi}} \frac{(1-\nu)}{\nu^2}. \quad (4.25)$$

The test of calculations were made for the value of the parameters $\nu = \frac{1}{2}, 1, 2$. Both schemes (Lax-Wendroff and upwind) were tested. For integration we tested different quadrature formulae. In the results we have chosen the quadrature formula based on the spline interpolation (see Appendix A). In these tests the following

parameters were used

$$\tau = 0.01, \quad h_x = \frac{1}{12}, \quad -8 \leq v_x < 8, \quad 0 < v_r \leq 8. \quad (4.26)$$

For the chosen parameters, the stability condition of the Lax-Wendroff and upwind schemes is satisfied, i.e., the Courant number is

$$\frac{\tau \cdot \max |v_x|}{h_x} = 0.96 < 1.$$

The number of samples points used on both v_x and v_r variables are 128.

For the parameter $\nu = 1$ the relative L_∞ -norm of error of the numerical solution and the hydrodynamic parameters were less than 10^{-5} over the time interval $t \leq 1$.

For the parameter $\nu = 2$ the relative L_∞ -norm of error of the numerical solution and the hydrodynamic parameters were less than 10^{-4} over the same time interval (10^{-3} for U_x). The values of the hydrodynamic moments for $t = 1.0$ are presented in Table 4.1. The error is mostly defined by the used quadrature

Table 4.1 Comparison between exact and numerical hydrodynamic variables

moments	exact	$x = -0.5$	$x = 0.0$	$x = 0.5$
n	1	1.00001	0.999998	1.00001
nU_x	0	1.05133×10^{-3}	1.05025×10^{-3}	1.04382×10^{-3}
T	1	1.00001	1.00001	1
q_x	0.398942	0.398958	0.398957	0.398952

formula. Similar results were also obtained for $\nu = \frac{1}{2}$.

Analysis of calculations has shown that the Lax-Wendroff and upwind numerical scheme practically give the same results.

4.2.2 Testing the algorithm of the relaxation stage

First part of the splitting method consists of the next numerical procedures.

1. Computing of the initial data by the Fourier and Hankel transforms of the solution of the Boltzmann equation on the previous time layer $t = \tau_n$.
2. Solving the Cauchy problem

$$\begin{cases} \varphi_t = \hat{Q}(\varphi, \varphi), \\ \varphi(\tau_n) = FHT\{f(\tau_n)\}, \end{cases} \quad (4.27)$$

for all grid point of the time layer $t = \tau_n$.

3. Calculating the inverse Fourier and Hankel transforms of the found solution $\varphi(t_n + \tau)$. The results give us data for the second stage of the splitting method.

All these procedures were tested with the well-known exact solutions of the space homogeneous Boltzmann equation. In these tests the following parameters were used

$$\tau = 0.05, \quad -8 \leq v_x, k_x < 8, \quad 0 < v_r, k_r \leq 8. \quad (4.28)$$

The number of sample points used on v_x and v_r variables are 256 and 2048 respectively. The number of sample points used on the variables of integration α, μ in the collision integral (2.77) are both 16.

The first was the Maxwell solution

$$f(\mathbf{v}, t) = \frac{1}{(2\pi)^{\frac{3}{2}}} e^{-\frac{\mathbf{v}^2}{2}}, \quad (4.29)$$

which is the stationary solution of the problem nullifying the collision integral. Its Fourier and Hankel transform has the form

$$\varphi(\mathbf{k}, t) = e^{-2\pi^2 \mathbf{k}^2}. \quad (4.30)$$

Table 4.2 shows the comparison between the exact and numerical solution in the L_∞ -norm of error.

Table 4.2 Comparison between exact (Maxwell solution) and numerical solution (relative L_∞ -norm of error), $\tau = 0.05$.

	$t = \tau$	$t = 2\tau$	$t = 3\tau$	$t = 4\tau$	$t = 5\tau$
$\ \hat{Q}(\varphi, \varphi) - \hat{Q}(\tilde{\varphi}, \tilde{\varphi})\ _\infty$	3.3×10^{-3}	3.3×10^{-3}	3.4×10^{-3}	3.4×10^{-3}	3.4×10^{-3}
$\ \varphi - \tilde{\varphi}\ _\infty$	3.7×10^{-3}	3.8×10^{-3}	3.9×10^{-3}	4.0×10^{-3}	4.0×10^{-3}
$\ f - \tilde{f}\ _\infty$	2.1×10^{-3}	2.1×10^{-3}	2.2×10^{-3}	2.2×10^{-3}	2.3×10^{-3}

The second solution was the Bobylev-Krook-Wu (BKW) solution

$$f(\mathbf{v}, t) = \frac{(2\pi)^{3/2}}{(1-\theta)^{3/2}} e^{-\frac{(2\pi)^2}{2(1-\theta)}|\mathbf{v}|^2} \left[1 + \frac{\theta}{1-\theta} \left(\frac{(2\pi)^2}{2(1-\theta)}|\mathbf{v}|^2 - \frac{3}{2} \right) \right], \quad \theta = 0.4e^{-t/6}. \quad (4.31)$$

for which the collision integral is not equal to zero. Its Fourier and Hankel transforms has the form

$$\varphi(\mathbf{k}, t) = (1 - 0.2\mathbf{k}^2 e^{-\frac{t}{6}}) e^{-\frac{\mathbf{k}^2}{2} + 0.2\mathbf{k}^2 e^{-\frac{t}{6}}}. \quad (4.32)$$

These function are characteristic distributions for the problems studied in the thesis. This allowed checking procedures 1, 2 and 3. The typical results for BKW can be seen in Table 4.3.

For numerical integration of the Cauchy problem (4.27), we tested the Runge-Kutta schemes of the first, second and fourth orders. The most part of the tests were made with using the BKW solution (4.31). Calculations have shown that the second and fourth order scheme took unreasonable computing time. Thus, for further calculations, we chose the first order Runge-Kutta scheme (Euler's method). The essential moment of the realization of the Runge-Kutta scheme (3.21) both with respect to the volume of calculations and computational precision is computing the collision integral. Because of that we separately tested the computing procedure for the collision integral.

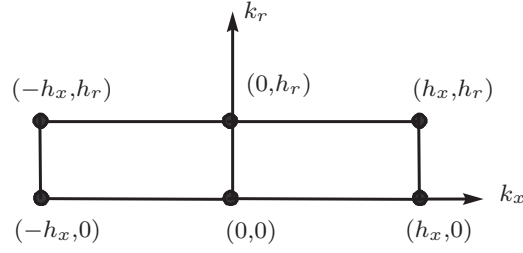


Figure 4.1 Stencil for asymptotic approximation.

The time derivative of the BKW solution is the collision integral and expressed as follows,

$$\varphi_t(\mathbf{k}, t) = \hat{Q}(\varphi, \varphi)(\mathbf{k}, t) = \frac{0.04}{6} |\mathbf{k}|^4 e^{\left(-\frac{t}{3} + \mathbf{k}^2 \left(-\frac{1}{2} + 0.2e^{-\frac{t}{6}}\right)\right)}. \quad (4.33)$$

Comparisons of the results of calculations with the exact solution in the relative L_∞ -norm of error are presented in Table 4.3.

Table 4.3 Comparison between exact (BKW solution) and numerical solution (relative L_∞ -norm of error), $\tau = 0.05$.

	$t = \tau$	$t = 2\tau$	$t = 3\tau$	$t = 4\tau$	$t = 5\tau$
$\ \hat{Q}(\varphi, \varphi) - \hat{Q}(\tilde{\varphi}, \tilde{\varphi})\ _\infty$	4.8×10^{-4}	9.5×10^{-4}	1.4×10^{-3}	1.8×10^{-3}	2.2×10^{-3}
$\ \varphi - \tilde{\varphi}\ _\infty$	2.9×10^{-5}	5.5×10^{-5}	8.1×10^{-5}	1.0×10^{-4}	1.2×10^{-4}
$\ f - \tilde{f}\ _\infty$	1.0×10^{-3}	1.9×10^{-3}	2.7×10^{-3}	3.5×10^{-3}	4.3×10^{-3}

On the relaxation stage, it is important to satisfy the conservation laws of mass, momentum and energy. For this purpose, we used asymptotic solution of the relaxation problem near zero grid point (Section 3.5.3). Conservation laws in the discrete form are expressed through finite differences, which are calculated on the grid stencil as shown in Figure 4.1.

4.3 Heat transfer problem between parallel plates

The heat transfer problem is a classical problem in rarefied gas dynamics. Despite of its simplicity it is included as a part of more complex problems. From the computational point of view, it is of interest because all numerical methods used in rarefied gas dynamics were tested by this problem. This problem is set as the following. Monatomic gas is contained between two parallel plates separated by a distance L . The plates have fixed temperatures T_1 and T_2 , $T_1 \leq T_2$. It is assumed that on the plates, complete accommodation of momentum and energy takes place. Molecules out going from the plates have half-space Maxwellian distributions with temperature T_1 and T_2 . In the dimensionless variables introduced earlier (3.4), the boundary conditions have the form (3.7)

$$\begin{cases} f(\frac{1}{2}, v_x, v_r) = n_+ (2\pi T_+)^{-\frac{3}{2}} e^{-\frac{(v_x^2+v_r^2)}{2T_+}}, & v_x < 0, \\ f(-\frac{1}{2}, v_x, v_r) = n_- (2\pi)^{-\frac{3}{2}} e^{-\frac{(v_x^2+v_r^2)}{2}}, & v_x > 0. \end{cases} \quad (4.34)$$

The stationary solution of the problem is obtained by an iterative method based on the described splitting method. The initial data that we used were the free molecular solution (4.22). The parameters of the problem are the Knudsen number

$$Kn = \frac{1}{\bar{n}\sigma_0 L \sqrt{\frac{kT_1}{m}}},$$

and the ratio of the temperatures

$$T_+ = \frac{T_2}{T_1}.$$

In our calculations, the Knudsen number was chosen as

$$Kn = \frac{1}{20\sqrt{2}}, \frac{1}{4}, \frac{1}{2\sqrt{2}}, 1.0.$$

The ratio of temperatures which we used was

$$T_+ = 4.$$

Such values of the parameters were considered in many papers where this problem was studied (Aristov, Ivanov and Tcheremissine, 1991 and references therein).

In the calculations of the heat transfer problem, the grid parameters coincide with the parameters chosen in the tests. Convergence of the density and temperature profiles for $Kn = \frac{1}{2\sqrt{2}}$ and $Kn = 1.0$ are shown in the Figure 4.2–4.5.

The maximal time values on the graphs correspond to obtained stationary solutions. Additional control of convergency was considered through the behavior of the profiles of the mean velocity U_x and the heat flux q_x . In the stationary solution the mean velocity $U_x = 0$ and the heat flux is constant. These data are presented in Table 4.4. There are numerous data for the hard sphere model (Aristov, Ivanov and Tcheremissine, 1991 and references therein). However, this model is opposite to the model of Maxwellian molecules with respect to “rigidity” of molecular collisions. Hence, one cannot expect that the profiles of the distribution function and even of the hydrodynamic variables, for example, n, T, q_x , of the two models coincide. For this reason the estimates of qualitative behavior of the profiles for these two molecule models (Section 4.1) and for different Knudsen numbers were made. Examples of comparison are presented in Figure 4.6 and Figure 4.7. The shearing of the distribution function which is defined by

$$\bar{f}(x, v_x) = 2\pi \int_R v_r f(x, v_x, v_r) dv_r$$

was compared for the case $x = 0$ as shown in Figure 4.8. Comparison were made for the following Knudsen number relations

$$Kn_M = \frac{1}{2\sqrt{2}} Kn_S.$$

This relation follows from the comparison of the dimensionless forms of the Boltzmann equation for these models. On one hand one can see that in general the total behavior of macroscopic parameters is similar for both models for the Knudsen

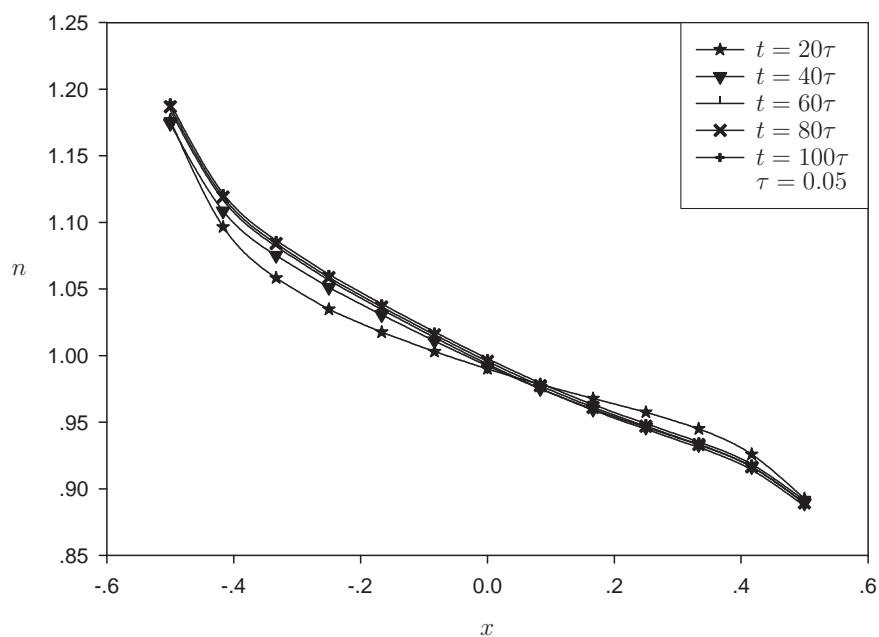


Figure 4.2 Convergence of the density profiles for $Kn = \frac{1}{2\sqrt{2}}$

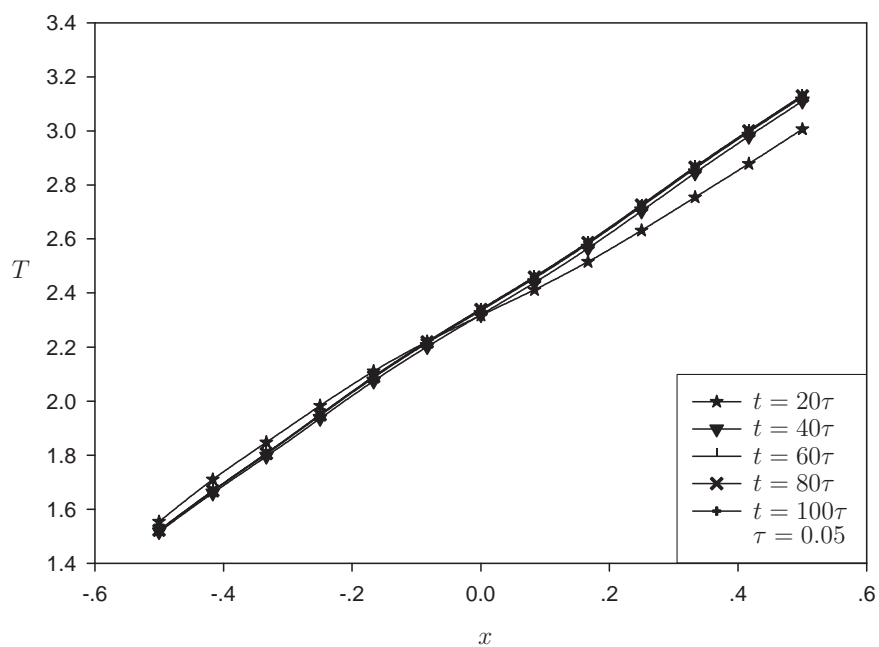


Figure 4.3 Convergence of the temperature profiles for $Kn = \frac{1}{2\sqrt{2}}$

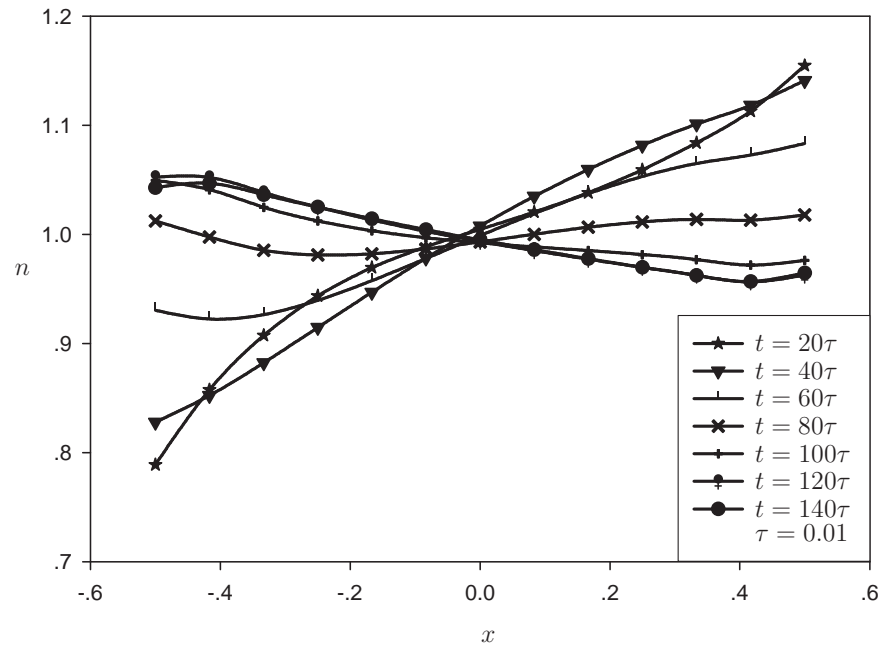


Figure 4.4 Convergence of the density profiles for $Kn = 1.0$

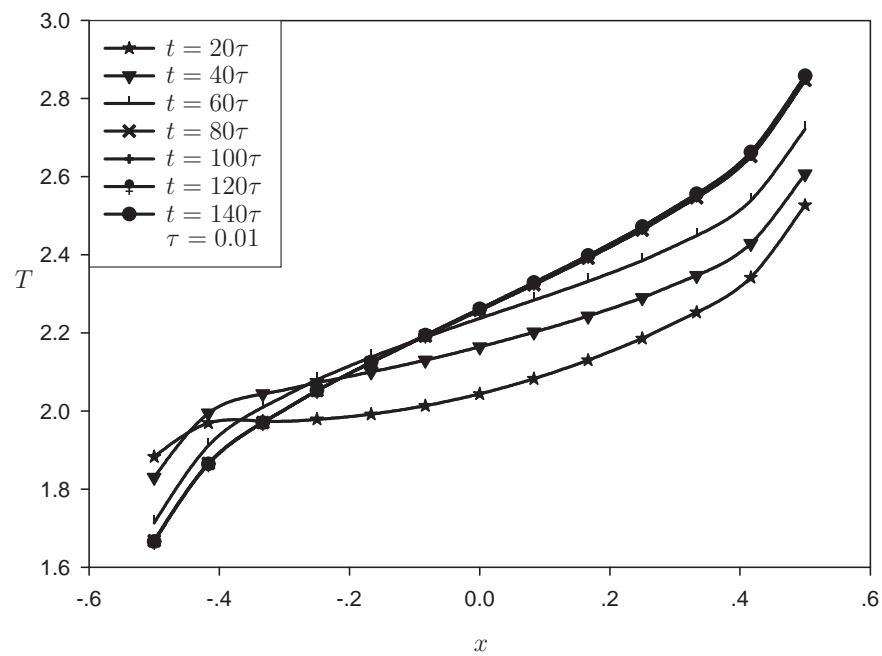


Figure 4.5 Convergence of the temperature profiles for $Kn = 1.0$

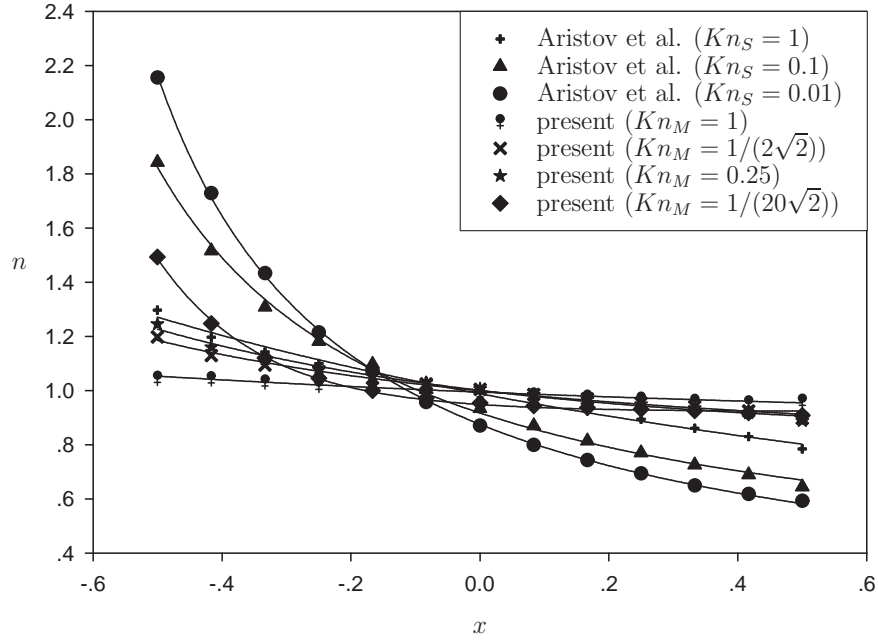


Figure 4.6 Density profiles for different Knudsen number. $Kn_S = 0.01, 0.1, 1$;
 $Kn_M = \frac{1}{20\sqrt{2}}, 0.25, \frac{1}{2\sqrt{2}}, 1$.

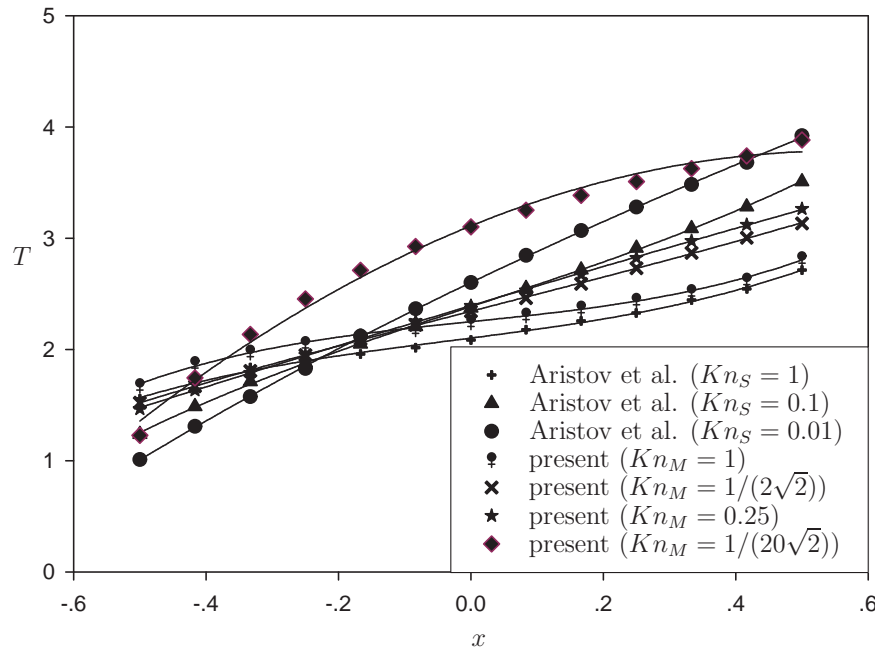


Figure 4.7 Temperature profiles for different Knudsen number. $Kn_S = 0.01, 0.1, 1$;
 $Kn_M = \frac{1}{20\sqrt{2}}, 0.25, \frac{1}{2\sqrt{2}}, 1$.

Table 4.4 Mean velocity and heat flux at the stationary solution for $Kn_M = 1$ (Maxwell model).

x	U_x	q_x
-0.50000	-4.84805×10^{-5}	-1.83775
-0.41667	-1.74364×10^{-3}	-1.49964
0 -.33333	-2.15324×10^{-3}	-1.43969
-0.25000	-2.31867×10^{-3}	-1.41967
-0.16667	-2.38621×10^{-3}	-1.41029
-0.08333	-2.38777×10^{-3}	-1.40512
0 0.00000	-2.33261×10^{-3}	-1.40233
0 .08333	-2.22379×10^{-3}	-1.40147
0 .16667	-2.06102×10^{-3}	-1.40299
0 .25000	-1.83784×10^{-3}	-1.40865
0 .33333	-1.52634×10^{-3}	-1.42432
0 .41667	-1.00204×10^{-3}	-1.47421
0 .50000	4.19422×10^{-4}	-1.75050

numbers considered. At the same time the difference in the profile inclines corresponds to the obtained estimates (Section 4.1.1).

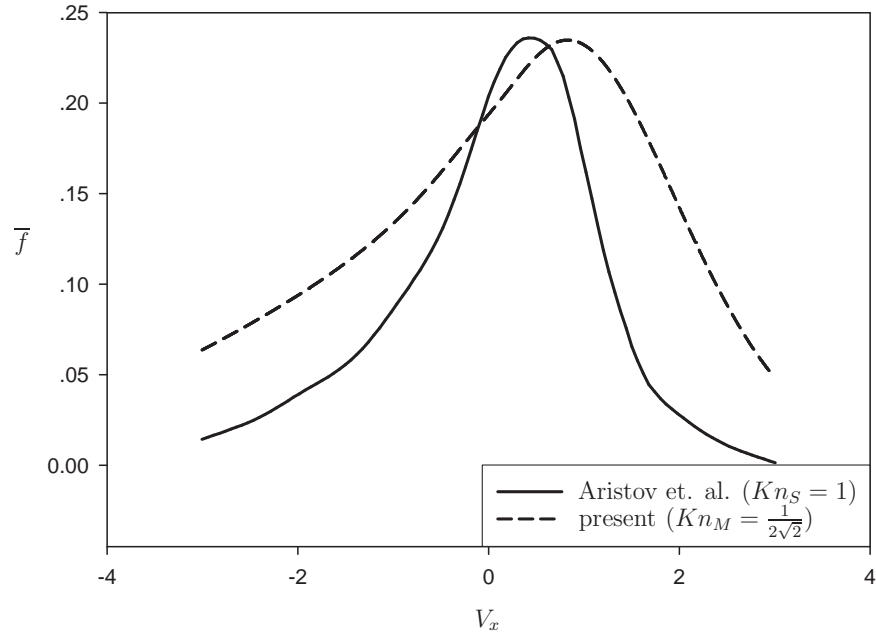


Figure 4.8 Comparison of the shearing of the distribution function

4.4 Recondensation between parallel plates

The “hot” plate at $x = -\frac{L}{2}$ emits molecules with the Maxwellian distribution function defined by the temperature T_1 and the density n_1 . The values n_1 and T_1 are given. On the “cold” plate at $x = \frac{L}{2}$, complete or partial condensation is characterized by the sorbtion coefficient $\beta \in [0, 1]$. The value $\beta = 0$ corresponds to the case when all coming molecules are sorbed, and maximal mass flow takes place. The value $\beta = 1$ corresponds to the case where all coming molecules are reflected from the plate. Complete or partial reflection occurs with the Maxwellian distribution function defined by the given temperature $T_2 \leq T_1$. The density of reflected molecules n_2 is defined by the equality

$$N_r = \beta N_i,$$

where N_i is a flux of incoming molecules and N_r is a flux of reflected molecules.

For dimensional analysis of the problem we chose the next characteristic

values: the length L , the density n_1 , the temperature of the “cold” plate T_2 , molecular velocity $v_0 = \sqrt{\frac{kT_2}{m}}$ and the distribution function $f_0 = n_1 v_0^{-3}$. The recondensation problem for the Boltzmann equation

$$v_x \frac{\partial f}{\partial x} = \frac{1}{4\pi k n} \int_{\mathbb{R}^3} \int_{S^2} [f(\mathbf{v}')f(\mathbf{v}_1) - f(\mathbf{v})f(\mathbf{v}_1)] d\mathbf{n} d\mathbf{v}_1, \quad (4.35)$$

has the boundary condition

$$\begin{cases} f(\frac{1}{2}, v_x, v_r) = n_2 (2\pi)^{-\frac{3}{2}} e^{-\frac{(v_x^2 + v_r^2)}{2}}, & v_x < 0, \\ f(-\frac{1}{2}, v_x, v_r) = (2\pi\mu)^{-\frac{3}{2}} e^{-\frac{(v_x^2 + v_r^2)}{2\mu}}, & v_x > 0, \end{cases} \quad (4.36)$$

where $\mu = \frac{T_1}{T_2}$, $n_2 = (2\pi)^{\frac{3}{2}} \beta \int_0^\infty \int_0^\infty v_x v_r f(\frac{1}{2}, v_x, v_r) dv_r dv_x$.

For the stationary solution, the mass flux q_m and the moment flux q_x along the x -axis are constant:

$$q_m(x) = 2\pi \int_{-\infty}^\infty \int_0^\infty v_x v_r f(x, v_x, v_r) dv_r dv_x, \quad (4.37)$$

$$q_x(x) = 2\pi \int_{-\infty}^\infty \int_0^\infty v_x^2 v_r f(x, v_x, v_r) dv_r dv_x. \quad (4.38)$$

Since this problem differ only slightly in boundary conditions from the heat transfer problem, it can be easily computed by the developed code. As for example, convergence of the density and temperature profiles for $\beta = 0$, $\mu = 4$ and $Kn = 0.125$ are presented in Figures 4.9–4.10.

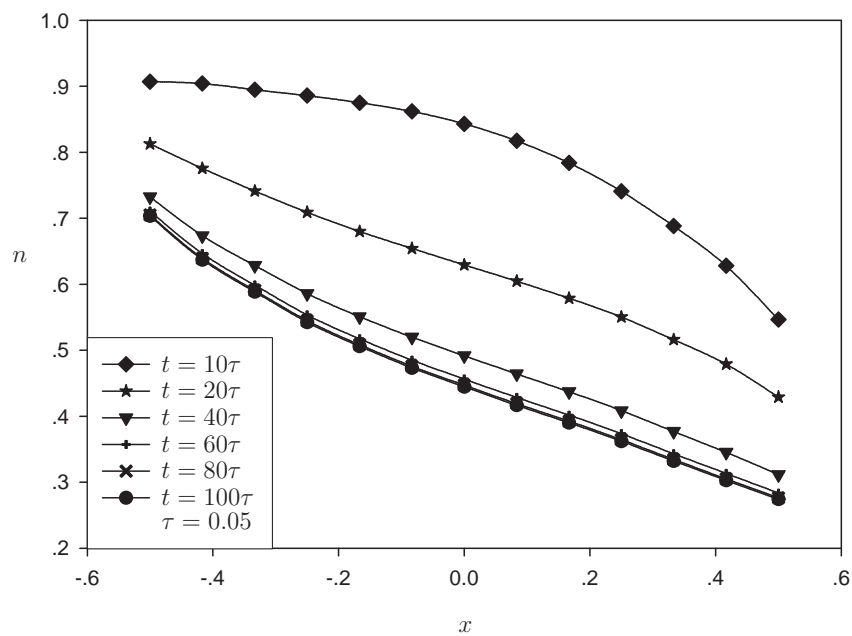


Figure 4.9 Convergence of the density profiles for $Kn = 0.125$

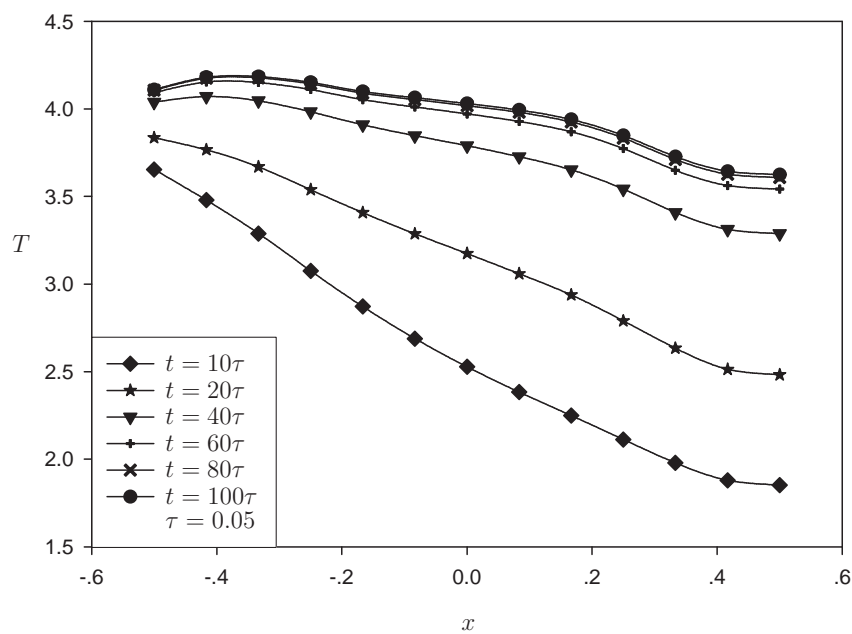


Figure 4.10 Convergence of the temperature profiles for $Kn = 0.125$

4.5 Conclusion

The new deterministic numerical method for solving the Boltzmann equation in the case of Maxwell molecule was developed. The method is based on the splitting scheme with respect to physical processes. The main feature of the method is the use of the Fast Fourier and Hankel procedures which defines efficiency of the method estimated as $O(N \log_2 N)$. All parts of the algorithm were carefully tested with exact solutions. As a sample application of the proposed method, the classical problem of heat transfer between two parallel plates was calculated for a wide interval of the Knudsen numbers. The results of calculations confirmed a good availability of the created mathematical tools. The developed code can be applied to many other similar problems of the gas kinetic theory.

REFERENCES

REFERENCES

- Aristov, V. V., Ivanov M. S. and Tcheremissine F. G. (1991). Solution of the problem on one-dimensional heat transfer in a rarefied gas by two methods. **USSR J. Comp. Math. Math. Phys.** 31: 623-626.
- Bird, G. A. (1976). **Molecular Gas Dynamics**. Oxford: Clarendon Press.
- Bobylev, A. V. (1975). The method of Fourier transform in the theory of the Boltzmann equation for Maxwell molecules. **Dokl. Akad. Nauk SSSR.** 225: 1041-1044.
- Bobylev, A. V. and Rjasanow, S. (1997). Difference scheme for the Boltzmann equation based on the fast Fourier transform. **Eur. J. Mech. B/Fluids** 16: 293306.
- Brigham, E. O. (1974). **The fast Fourier transform**. USA: Prentice-Hall, Inc.
- Cercignani, C. (1975). **Theory and Application of the Boltzmann Equation**. New York: Elsevier.
- Cercignani, C. (1988). **The Boltzmann Equation and Its Applications**. New York: Springer-Verlag.
- Cercignani, C. (2000). **Rarefied Gas Dynamics From Basic Concepts to Actual Calculations**. Cambridge: Cambridge University Press.
- Cooley, J. W. and Turkey, J. W. (1965). An algorithm for machine calculation of complex Fourier series. **Math. Comp.** 19: 297-301.

- Grigoriev, Y. N. and Mikhalitsyn, A. N. (1985). Nonmonotone relaxation in an atomic gas and kinetics of threshold processes. **J. Appl. Mech. Tech. Phys.** 5: 6-14.
- Grigoriev, Y. N. and Mikhalitsyn, A. N. (1985). A spectral method of solving Boltzmann's kinetic equation numerically. **USSR J. Comp. Math. Math. Phys.** 23 (6): 105-111.
- Kogan, M. N. (1969). **Rarefied Gas Dynamics**. New York: Plenum Press.
- Luke, Y. L. (1962). **Integral of Bessel Functions**. USA: McGraw-Hill.
- Nanbu, K. (1983). Direct simulation scheme derived from the Boltzmann equation. **I. Monocomponent Gases, J. Phys. Soc. Japan.** 52: 2042-2049.
- Pareschi, L. and Russo, G. (2000). Numerical solution of the Boltzmann equation. I. Spectrally accurate approximation of the collision operator. **Siam J. Numer. Anal.** 37 (4): 1217-1245.
- Poularikas, A. D. (1996). **The Transform and Applications Handbook**. CRC Press.
- Siegman, A. E. (1977). Quasi-fast Hankel transform. **Opt. Lett.** 1: 13-15.
- Sneddon, I. N. (1972). **The Use of Integral Transforms**. USA: McGraw-Hill, Inc.

APPENDICES

APPENDIX A

CUBIC SPLINE INTERPOLATION AND QUADRATURE

Given a tabulate function $y_j = y(x_j)$, $j = 0, \dots, n - 1$, we seek a piecewise continuous function, passing through each of these values. A cubic spline function is an ordered set of cubic polynomials which match up smoothly and form a twice continuously differentiable function. According to “numerical recipes in c++ : the art of scientific computing” (William H. Press, Saul A. Teukolsky, William T. Vetterling and Brian P. Flannery, 2002), a cubic spline interpolation on interval (x_j, x_{j+1}) is given by

$$y = Ay_j + By_{j+1} + Cy_j'' + Dy_{j+1}'', \quad (\text{A.1})$$

where

$$\begin{aligned} A &= \frac{x_{j+1} - x}{x_{j+1} - x_j} \\ B &= 1 - A \\ C &= \frac{(A^3 - A)(x_{j+1} - x_j)^2}{6} \\ D &= \frac{(B^3 - B)(x_{j+1} - x_j)^2}{6} \end{aligned} \quad (\text{A.2})$$

The requirement that the first and second derivative must be continuous lead to the following system of equations

$$\frac{x_j - x_{j-1}}{6} y_{j-1}'' + \frac{x_{j+1} - x_{j-1}}{3} y_j'' + \frac{x_{j+1} - x_j}{6} y_{j+1}'' = \frac{y_{j+1} - y_j}{x_{j+1} - x_j} - \frac{y_j - y_{j-1}}{x_j - x_{j-1}},$$

$$j = 1, \dots, n - 2. \quad (\text{A.3})$$

These are $n-2$ linear equations in the n unknowns y''_i , $i = 0, \dots, n-1$. In order to solve this systems, we need two additional conditions. In this thesis, we impose the condition of continuity of the third derivative at the points adjacent to the endpoints of the interval, i.e., y'''_1 and y'''_{n-2} are continuous.

On the interval (x_j, x_{j+1}) , from (A.1), the third derivative is

$$y''' = \frac{y''_{j+1} - y''_j}{x_{j+1} - x_j}. \quad (\text{A.4})$$

The required condition yields

$$\frac{y''_1 - y''_0}{x_1 - x_0} = \frac{y''_2 - y''_1}{x_2 - x_1} \quad (\text{A.5})$$

and

$$\frac{y''_{n-2} - y''_{n-3}}{x_{n-2} - x_{n-3}} = \frac{y''_{n-1} - y''_{n-2}}{x_{n-1} - x_{n-2}}. \quad (\text{A.6})$$

Rearrangement of (A.5) and (A.6) yields

$$y''_0 = \frac{x_2 - x_0}{x_2 - x_1} y''_1 - \frac{x_1 - x_0}{x_2 - x_1} y''_2 \quad (\text{A.7})$$

$$y''_{n-1} = \frac{x_{n-1} - x_{n-3}}{x_{n-2} - x_{n-3}} y''_{n-2} - \frac{x_{n-1} - x_{n-2}}{x_{n-2} - x_{n-3}} y''_{n-3}. \quad (\text{A.8})$$

Substituting (A.7) and (A.8) into (A.3), we have a tridiagonal system of $n-2$ unknowns y''_i , $i = 1, \dots, n-2$,

$$\begin{bmatrix} b_0 & c_0 & 0 & \cdots & 0 & 0 & 0 \\ a_1 & b_1 & c_1 & \cdots & 0 & 0 & 0 \\ \vdots & \vdots & \vdots & \ddots & \vdots & \vdots & \vdots \\ 0 & 0 & 0 & \cdots & a_{N-4} & b_{N-4} & c_{N-4} \\ 0 & 0 & 0 & \cdots & 0 & a_{N-3} & b_{N-3} \end{bmatrix} \begin{bmatrix} y''_1 \\ y''_2 \\ \vdots \\ y''_{N-3} \\ y''_{N-2} \end{bmatrix} = \begin{bmatrix} r_0 \\ r_1 \\ \vdots \\ r_{N-4} \\ r_{N-3} \end{bmatrix} \quad (\text{A.9})$$

where

$$\begin{aligned}
a_{j-1} &= \frac{x_j - x_{j-1}}{6} \\
b_{j-1} &= \frac{x_{j+1} - x_{j-1}}{3} \\
c_{j-1} &= \frac{x_{j+1} - x_j}{6} \\
r_{j-1} &= \frac{y_{j+1} - y_j}{x_{j+1} - x_j} - \frac{y_j - y_{j-1}}{x_j - x_{j-1}}
\end{aligned}$$

for $j = 2, \dots, N - 3$ and

$$\begin{aligned}
b[0] &= \frac{(x_1 - x_0)(x_2 - x_0)}{6(x_2 - x_1)} + \frac{x_2 - x_0}{3} \\
c[0] &= -\frac{(x_1 - x_0)^2}{6(x_2 - x_1)} + \frac{x_2 - x_1}{6} \\
r[0] &= \frac{y_2 - y_1}{x_2 - x_1} - \frac{y_1 - y_0}{x_1 - x_0} \\
a[N - 3] &= \frac{x_{N-2} - x_{N-3}}{6} - \frac{(x_{N-1} - x_{N-2})^2}{6(x_{N-2} - x_{N-3})} \\
b[N - 3] &= \frac{x_{N-1} - x_{N-3}}{3} + \frac{(x_{N-1} - x_{N-2})(x_{N-1} - x_{N-3})}{6(x_{N-2} - x_{N-3})} \\
r[N - 3] &= \frac{y_{N-1} - y_{N-2}}{x_{N-1} - x_{N-2}} - \frac{y_{N-2} - y_{N-3}}{x_{N-2} - x_{N-3}}.
\end{aligned}$$

For derivation of the cubic spline quadrature formula, we directly integrate the cubic spline function obtained by (A.1) on the interval (x_j, x_{j+1}) ,

$$\int_{x_j}^{x_{j+1}} y dx = y_j \int_{x_j}^{x_{j+1}} A dx + y_{j+1} \int_{x_j}^{x_{j+1}} B dx + y_j'' \int_{x_j}^{x_{j+1}} C dx + y_{j+1}'' \int_{x_j}^{x_{j+1}} D dx. \quad (\text{A.10})$$

By using (A.2), we obtain

$$\begin{aligned}
\int_{x_j}^{x_{j+1}} A dx &= \frac{x_{j+1} - x_j}{2} \\
\int_{x_j}^{x_{j+1}} B dx &= \frac{x_{j+1} - x_j}{2} \\
\int_{x_j}^{x_{j+1}} A^3 dx &= \frac{x_{j+1} - x_j}{4} \\
\int_{x_j}^{x_{j+1}} B^3 dx &= \frac{x_{j+1} - x_j}{4}.
\end{aligned} \quad (\text{A.11})$$

Substituting (A.11) into (A.10), we have

$$\int_{x_j}^{x_{j+1}} y dx = \frac{(x_{j+1} - x_j)(y_j + y_{j+1})}{2} - \frac{(x_{j+1} - x_j)^3(y_j'' + y_{j+1}'')}{24}. \quad (\text{A.12})$$

APPENDIX B

CALCULATION OF SOME INTEGRALS

Here we give details of the calculations of integrals which we used in the section for estimating behavior of profiles of hydrodynamic variables.

Let us consider the integral

$$F_1 = \frac{1}{n^2} \int_{R^3} \int_{R^3} |\mathbf{v} - \mathbf{v}_1|^2 f_0(\mathbf{v}) f_0(\mathbf{v}_1) d\mathbf{v}_1 d\mathbf{v}. \quad (\text{B.1})$$

In our dimensionless variables

$$f_0(\mathbf{v}) = \frac{n}{(2\pi)^{\frac{3}{2}}} e^{-\frac{\mathbf{v}^2}{2}}. \quad (\text{B.2})$$

The change of variables

$$\mathbf{R} = \frac{1}{2}(\mathbf{v} + \mathbf{v}_1), \quad \mathbf{g} = \mathbf{v} - \mathbf{v}_1, \quad (\text{B.3})$$

is a linear orthogonal transformation. Thus one has

$$d\mathbf{v}d\mathbf{v}_1 = d\mathbf{R}d\mathbf{g}.$$

From the change, we have

$$\mathbf{v} = \mathbf{R} + \frac{1}{2}\mathbf{g}, \quad \mathbf{v}_1 = \mathbf{R} - \frac{1}{2}\mathbf{g}. \quad (\text{B.4})$$

This change gives

$$F_1 = \frac{1}{(2\pi)^3} \int_{R^3} \int_{R^3} |\mathbf{g}|^2 e^{-\mathbf{R}^2} e^{-\frac{\mathbf{g}^2}{4}} d\mathbf{R}d\mathbf{g}. \quad (\text{B.5})$$

Using spherical coordinates

$$d\mathbf{R} = \rho^2 \sin \theta d\theta d\varphi d\rho, \quad (\text{B.6})$$

$$d\mathbf{g} = \rho_1^2 \sin \theta_1 d\theta_1 d\varphi_1 d\rho_1, \quad (\text{B.7})$$

the six-dimensional integral becomes

$$\begin{aligned}
 F_1 &= \frac{1}{(2\pi)^3} \int_0^\pi \sin \theta d\theta \int_0^\pi \sin \theta_1 d\theta_1 \int_0^{2\pi} d\varphi \int_0^{2\pi} d\varphi_1 \int_0^\infty \rho^2 e^{-\rho^2} d\rho \int_0^\infty \rho_1^4 e^{-\frac{\rho_1^2}{4}} d\rho_1 \\
 &= \frac{2}{\pi} \int_0^\infty \rho^2 e^{-\rho^2} d\rho \int_0^\infty \rho_1^4 e^{-\frac{\rho_1^2}{4}} d\rho_1.
 \end{aligned} \tag{B.8}$$

The last two integrals are (Kogan, 1969)

$$\int_0^\infty \rho^2 e^{-\rho^2} d\rho = \frac{\sqrt{\pi}}{4}, \tag{B.9}$$

$$\int_0^\infty \rho_1^4 e^{-\frac{\rho_1^2}{4}} d\rho_1 = 12\sqrt{\pi}. \tag{B.10}$$

As the result, we obtain

$$F_1 = 6. \tag{B.11}$$

Another integral is

$$\begin{aligned}
 I_2 &= \int_{R^3} \int_{R^3} \int_{S^2} f_0(\mathbf{v}) f_0(\mathbf{v}_1) |\mathbf{v} - \mathbf{v}_1| d\mathbf{n} d\mathbf{v}_1 d\mathbf{v} \\
 &= \frac{n^2}{4\pi^2} \int_{R^3} \int_{R^3} e^{-\frac{v^2 + v_1^2}{2}} |\mathbf{v} - \mathbf{v}_1| d\mathbf{v}_1 d\mathbf{v} \\
 &= 4n^2 \int_0^\infty \rho^2 e^{-\rho^2} d\rho \int_0^\infty \rho_1^3 e^{-\frac{\rho_1^2}{4}} d\rho_1 \\
 &= 8\sqrt{\pi} n^2.
 \end{aligned} \tag{B.12}$$

APPENDIX C

INTEGRAL IDENTITY

Here we show the integral identity

$$\int_{S^2} e^{-i2\pi|\mathbf{u}|\mathbf{k}\cdot\mathbf{n}/2} d\mathbf{n} = \int_{S^2} e^{-i2\pi|\mathbf{k}|\mathbf{u}\cdot\mathbf{n}/2} d\mathbf{n}, \quad (\text{C.1})$$

which we used for obtaining the Fourier transform of the space homogeneous Boltzmann equation.

Let us write

$$\mathbf{u} = |\mathbf{u}| \mathbf{n}_{\mathbf{u}}, \quad \mathbf{k} = |\mathbf{k}| \mathbf{n}_{\mathbf{k}}, \quad (\text{C.2})$$

where $\mathbf{n}_{\mathbf{u}}, \mathbf{n}_{\mathbf{k}}$ are unit vector on the sphere S^2 . There is the matrix of rotation A such that

$$\mathbf{n}_{\mathbf{u}} = A \mathbf{n}_{\mathbf{k}}. \quad (\text{C.3})$$

Then

$$\begin{aligned} \int_{S^2} e^{-i2\pi|\mathbf{u}|\mathbf{k}\cdot\mathbf{n}/2} d\mathbf{n} &= \int_{S^2} e^{-i2\pi|\mathbf{u}||\mathbf{k}|\mathbf{n}_{\mathbf{k}}\cdot\mathbf{n}/2} d\mathbf{n} \\ &= \int_{S^2} e^{-i2\pi|\mathbf{u}||\mathbf{k}|\mathbf{n}_{\mathbf{k}}\cdot A^{-1}\mathbf{n}/2} d\mathbf{n} \quad (\text{by substitution of } \mathbf{n} \text{ with } A^{-1}\mathbf{n}) \\ &= \int_{S^2} e^{-i2\pi|\mathbf{u}||\mathbf{k}|A\mathbf{n}_{\mathbf{k}}\cdot\mathbf{n}/2} d\mathbf{n} \\ &= \int_{S^2} e^{-i2\pi|\mathbf{u}||\mathbf{k}|\mathbf{n}_{\mathbf{u}}\cdot\mathbf{n}/2} d\mathbf{n} \\ &= \int_{S^2} e^{-i2\pi|\mathbf{k}|\mathbf{u}\cdot\mathbf{n}/2} d\mathbf{n}. \end{aligned}$$

CURRICULUM VITAE

NAME: Chatchawan Watchararuangwit.

GENDER: Male.

NATIONALITY: Thai.

DATE OF BIRTH: September 4, 1976.

EDUCATIONAL BACKGROUND:

- B.Sc. in Mathematics (Second Class Honors), Chiang Mai University, Chiang Mai, Thailand, 1998.
- M.Sc. in Applied Mathematics, Mahidol University, Bangkok, Thailand, 2002.

PUBLICATIONS:

- Watchararuangwit, C., Grigoriev Yu. N., Meleshko S. V. (2007). Application of the Hankel Transform for Solving the Boltzmann Equation with Cylindrical Symmetry. The 3rd IMT-GT 2007 Regional Conference on Mathematics, Statistics and Applications. Penang, Malaysia.
- Watchararuangwit, C., Grigoriev Yu. N., Meleshko S. V. (2007). Numerical solution of the Boltzmann equation with cylindrical symmetry. The 33rd Congress on Science and Technology of Thailand 2007. Walailak University, Thailand.
- Watchararuangwit, C., Grigoriev Yu. N., Meleshko S. V. (2007). Development of a deterministic spectral method for solving the nonlinear Boltzmann kinetic equation. Science Asia (submitted).

SCHOLARSHIPS:

- Royal Golden Jubilee Ph.D. Program, 2005-2007.
- Development and Promotion of Science and Technology Talents Project of Thailand (DPST), 1992-2004.